Article

Secrets of Kleiber's and Maximum Metabolic Rate Allometries Revealed with a Link to Oxygen-Deficient - Combustion -Engineering

Kalyan Annamalai *

Posted Date: 5 March 2025

doi: 10.20944/preprints202503.0386.v1

Keywords: Metabolism; Kleiber's Law; Oxygen Deficiency; Maximum Metabolic Rate; Organ-GOD Number

 doi:10.20944/preprints202503.0386.v1

Article

Secrets of Kleiber's and Maximum Metabolic Rate Allometries Revealed with a Link to Oxygen-Deficient -Combustion -Engineering

Kalyan Annamalai

Emeritus Prof., J. Mike Walker '66 Department of Mechanical Engineering, Texas A&M University, College Station, Texas 77845; k-annamalai@tamu.edu

Abstract: The biology literature addresses two puzzles: i) the increase in specific metabolic rate of organs (SOrMR, W/kg of organ) with a decrease in body mass (M_B) of biological species (BS), and ii) how the organs recognize they are in a smaller or larger body and adjust metabolic rates of the body ($\dot{q}_B$) accordingly. These puzzles were answered in the author's earlier work by linking the field of oxygen-deficient combustion (ODC) of fuel-particle clouds (FC) in engineering to the field of oxygen-deficient metabolism (ODM) of cell clouds (CC) in biology. The current work extends the ODM hypothesis to predict the whole body metabolic rates of 114 BS and demonstrates Kleiber's power law {$\dot{q}_B = a\ M_B^{\ b}$}. The methodology involves the i) extension of the effectiveness factor relation, expressed in terms of the dimensionless group number G (= Thiele Modulus^2), from engineering to the organs of BS, ii) modification of G as G_{OD} for the biology literature as a measure of oxygen deficiency (OD), iii) collection of data on organ and body masses of 116 species and prediction of $SOrMR_k$ of organ *k* of 114 BS using only the $SorMR_k$ of two reference species (Shrew, 0.0076 kg: RS-1; Rat, 0.380 kg: RS-2), iv) estimation of $\dot{q}_B$ of 114 species versus M_B and demonstration of Kleiber's law with a = 2.962, b = 0.747, and v) extension of ODM to predict the allometric law for maximal metabolic rate (MMR under exercise, {$\dot{q}_{B,MMR} = a_{MMR}\ M_B^{\ b_{MMR}}$}.) and validate the approach for MMR by comparing b_{MMR} with the literature data.

Keywords: metabolism; Kleiber's law; oxygen deficiency; maximum metabolic rate; organ-GOD number

1. Introduction, Literature Review and Objectives

Recent efforts aim to connect thermodynamics and combustion with biology to better understand the virus evolution, develop empirical formulae for viruses, and analyze biological processes through Gibbs function and energy release within biological systems (BS) [1–3]. This study extends previous work linking the field of oxygen-deficient combustion (ODC) with oxygen-deficient metabolism (ODM) [3] to predict the specific organ metabolic rates ($SorMR_k$) of vital organ *k* of mass m_k (W/kg of k, k= Kidneys (Kids), Heart, Brain and Liver) of 114 BS ranging in mass from 10 g to 6,650 kg by using i) data on $SorMR_k$ of two BS named as reference species (Shrew, 0.0076 kg: RS-1; Rat, 0.390 kg: RS-2), ii) data on organ masses of 116 species (114 +2 RS), and iii) established metabolic energy release relationships from ODC/porous char combustion literature. By summing the organ metabolic rates {MR} of individual organs ($OrMR_k$=$SorMR_k$ x m_k) across all organs, the whole-body metabolic rate (BMR) as a function of body mass (M_B) is obtained. The ODM approach is validated by demonstrating Kleiber's law and comparing the predicted allometric constants with literature data. The study provides a brief overview of Kleiber's law, followed by i) a review of current theories explaining the ¾-power law, ii) an introduction to ODC, the dimensionless group number G , ODM and corresponding G_{OD} # for organs, iv) the methodology adopted for the prediction of $SOrMR_k$ of

 doi:10.20944/preprints202503.0386.v1

114 species using only two RS, and v) validation and extension to allometry for maximal metabolic rate (MMR). A higher GOD # indicates a higher degree of oxygen deficiency.

1.1. Kleiber's Law and Organ Metabolic Rates

Allometry refers to how the characteristics of biological species (BS), including morphological traits (e.g., brain size) and physiological traits (e.g., metabolic rate (MR), life span), change with body mass. The allometric relation for MR in BS is given as:

$$\dot{q}_B = a \; M_B^{\;b} \tag{1}$$

where M_B is body mass (kg) and ($\dot{q}_B$), MR is in watts. In 1932, Kleiber obtained a = 3.4, b = 0.74 for M_B ranging from 0.15 to 679 kg, known as Kleiber's law [4,5], which persisted for over 70 years [6]. The specific basal metabolic rate (SBMR, W/kg of body mass) is written as

$$\dot{q}_{B,M} = a \; M_B \; b' \tag{2}$$

where b′ = b - 1 = -0.26

Nutrients consumed through the mouth are essential for energy release $\dot{q}_B$ through oxidation. The review in Ref. [8] suggests that O_2, which enters through nasal intake, must also be considered a "nutrient" since it is essential for energy release. The energy release rate (ERR) is related to the oxygen consumption rate $\{\dot{m}_{O2,B}\}$ within whole body since $ERR_B = \{\dot{m}_{O2,B}\} HHV_{O2}$, where HHV_{O2} t is the energy release per unit mass of oxygen consumed and it is almost constant at about 14335 J/g of O2 for most fuels and nutrients [1]. If O_2 supply falls below a critical level $\{\dot{m}_{O2,crit}\}$ then its uptake $\{\dot{m}_{O2}\}$ is limited by the supply from blood vessels, which is a common assumption used in the classical WBE {West, Brown and Enquist} hypothesis for demonstrating Kleiber's law.

The scaling function for metabolic rate with body size M_B is explained with two existing theories:

I). West et al. [7] proposed a fractal or "nutrient (including oxygen) distribution network" hypothesis (also referred to as the "upstream" or supply side [8] or "outward-directed vascular network" [9]) and illustrated Kleiber's law by minimizing the heart's work required to pump the unit amount of blood, i.e., a network which minimizes the pressure difference (P_{aorta}-P_{cap}). The scaling function is explained with O_2 delivery to cells as the limiting factor.

II). Bejan [10,11] proposed that architectures and organs must develop in such a way that resistance to flow current (e.g., water flow in trees) must be minimized, or equivalently, that entropy generation is minimized, resulting in lower energy consumption and food requirements.

The Biologists have raised the following issues as unknown: "The allometric size relationship is somehow 'programmed' into cells, although the factors that let them know whether they are in a small or large organism are still unknown" [12]. That is, existing biological data indicates that organs increase their metabolic rates per unit mass when within a smaller body and vice versa. In earlier work, the author proposed the "Oxygen-Deficient Metabolism (ODM)" hypothesis to explain these unknowns [3]. In the current work the same ODM hypothesis is extended to predict the specific organ metabolic rate of organ *k* {$SOrMR_k$, k= *k*= kidneys (kids), heart, brain and liver} of 114 BS ranging in mass from 10 g to 6,650 kg using data on $SOrMR_k$ of two reference BS { RS-1 of lowest M_B , Shrew, 7.5 g; RS-2 elected with M_B much higher than that of RS-1: Rat, 380 g }. With known vital organ masses m_k , the $OrMR_k$ {= $SOrMR_k \cdot m_k$} are estimated and summed up to yield the whole-body basal metabolic rate $\dot{q}_B$ as a function of body mass (M_B) for 116 BS ranging in mass from 0.0076 kg to 650 kg, The log-log plot yields Kleiber's law for 116 species ranging in mass from 0.007 kg to 650 kg, with an allometric exponent of b= 0.747. More importantly, the ODM presents a dimensionless group $(G_{OD})_k$ for biology literature to indicate the extent of OD within an organ.

 doi:10.20944/preprints202503.0386.v1

1.2. Literature Review

While combustion is a rapid oxidation process that typically occurs at high oxygen mass fraction, $Y_{O2,air}$ = 0.23 (mole fraction =0.21 or 23% or 210,000 ppm), resulting in a significant temperature rise, the metabolism is a slow oxidation process that typically occurs at a low oxygen mass fraction, Y_{O2} ($Y_{O_2} = 0.0415\, x\, p_{O_2}$ [13]), where p_{O2} is the partial pressure of O_2 in mm of Hg. While the pO2 in alveolar is 106 mm of Hg , the p_{O2} in tissues is about 40-50 mm Hg and dissolved O_2 is on the order of 1-6 ppm, thus resulting in a lower temperature rise. Sometimes, the biology literature calls $\dot{q}_B$ as "heat produced" or "power produced" [51], while the engineering literature defines $\dot{q}_B$ as the energy release rate (ERR) by all the cells within the body. The $\dot{q}_B$ is a sum of the work delivery rate, $\dot{W}_B$, (i.e., ATP delivery rate, approximately 25% of $\dot{q}_B$) and the heat transfer rate ($\dot{Q}_B$, approximately 75 % of $\dot{q}_B$, [52]) due to the temperature difference (ΔT) across the cells and the rest of the body.

The required O_2 uptake $\{\dot{m}_{O2}\}$ (biology uses volume units $\dot{V}_{O2}$ in mL/min, $\dot{m}_{O2}$ in mg/min=1.42 x $\dot{V}_{O2}$) by mitochondria in the cells is supplied by blood vessels via capillaries, followed by diffusion from capillaries to cells and then from cells to mitochondria.

The hypotheses used for demonstrating Kleiber's law { $\dot{q}_B$ vs M_B } fall under two broad groups: I) Homogeneous and II) Heterogeneous.

I). <u>Homogeneous hypothesis:</u>

This hypothesis considers the whole body as a system; the hypotheses include: i) the law of surface area to volume ratio of the whole body, yielding b=2/3, b'=-1/3, as described by Rubner's law in 1883, ii) WBE's fractal geometry [14] (geometry of circulatory system: macro and microcirculation), which relies on minimization of dissipative energy in the vascular system supplying oxygen and nutrients. Savage et al. showed that the WBE model is applicable only for BS of infinite body size (or network) [15], and when finite size is included, it yields scaling exponents as a function of body size. Further, Weibel and [16] question the universal models based on "the fractal design of the vasculature and the fractal nature of the total effective surface of mitochondria and capillaries" since they predict b= ¾ for both basal and maximal metabolic rates. Silva et al. [17] suggest that there are mathematical and conceptual errors in network models, weakening the proposed theoretical arguments. The same review suggests that the power law exponent *b* should vary between 2/3 and 1 based on 'metabolic level' (activity level of the organism or metabolic intensity). Painter et al. [18] agreed with the assumption of blood volume $\propto M_B$ but questioned the assumptions of uptake nutrient consumption rate (called total current in the network) proportional to blood volume, iii) network structures [9], iv) quantum mechanics [19], and v) topology [10].

II). <u>Heterogeneous Hypothesis:</u>

The heterogeneous hypothesis considers the whole-body metabolic rate $\dot{q}_B$ as a sum of the $OrMR_k$ with k= kids, H,Br,L and RM where RM represents all the remaining weakly metabolizing tissues. The mass of RM is given as

$$m_{RM} = M_B - m_{vit}, \quad m_{vit} = \sum m_k,\ k = Kids, H, Br, L$$

a) <u>Body Mass Based Allometry</u> Wang et al. used a heterogeneous or reductionist approach for estimating the whole-body metabolic rate { $\dot{q}_B$ } [20–22]:

$$\dot{q}_B = a\, M_B^{\ b} = \sum_k \dot{q}_{k,m}\, m_k, \quad M_B = \sum_k m_k, \quad k = Kids, H, Br, L, RM \tag{3}$$

 doi:10.20944/preprints202503.0386.v1

where $\dot{q}_{k,m}$ is the SOrMR$_k$ of kth organ { W/kg of k}given by the body mass based allometry (BMA) given by

$$\dot{q}_{k,m} = e_{k,6} M_B^{\,f_{k,6}}, \quad f_{k,6} < 0, \; k = Kids, H, Br, L, RM \tag{4}$$

Here afterwards, this method of computing SOrMR$_k$ using the empirical allometric relations (EAR) will be termed as EAR method. Wang et al. presented allometric relations for organ masses [21]:

$$m_k = c_{k,6} M_B^{\,d_{k,6}}, \; d_{k,6} > 0, \; k = Kids, H, Br, L, RM \tag{5}$$

Using Equation 4 and Equation 5 , the $\dot{q}_B$ is obtained as

$$\dot{q}_B = \sum_k \dot{q}_{k,m} \; m_k = \left(\sum_k c_{k,6} \, e_{k,6} \; M_B^{\,d_{k,6}+f_{k,6}} \right), \; k = Kids, H, Br, L, RM, \tag{6}$$

Based on data on the organ mass and $\dot{q}_{k,m}$ of six species (ranging from 0.48 kg of rat to 70 kg of human), Ref. [21] tabulates the constants $c_{k,6}$, $d_{k,6}$, $e_{k,6}$ and $f_{k,6}$. Table 1 tabulates the allometric constants $c_{k,6}$, $d_{k,6}$, $e_{k,6}$ and $f_{k,6}$. Since $d_{k,6}>0$, organ sizes are positively related to M_B, while the SOrMR$_k$, Equation 4) are negatively correlated with body mass ($f_{k,6}<0$). The additional subscript "6" indicates that the empirical constants are based on six species. As opposed to a majority of BS, , human brain masses are relatively larger, and the allometric relation underpredicts m_{Br} for humans. Thus, human brain mass is estimated using the encephalization quotient (EQ), which is the ratio of measured brain mass to the mass predicted with allometry. Gallagher et al. report that for a reference human of 70 kg [23], the RM for the 5-organ model is 66.2 kg, while the masses of Kids, H, Br, and L are 0.31, 0.33, 1.4 and 1.8 kg, respectively; this results in 94.5% of body mass being RM, while vital organs account for 5.5%. Each of these vital organs contribute 8.7% (Kids), 8.2% (Heart), 21.6% (Brain) and 20.2% (Liver) of the total BMR [24]. However, if one uses the data on $c_{k,6}$ and $d_{k,6}$ tabulated in Table 1, the resulting mass percentages are 0.37% (Kids), 0.58% (Heart), 0.40% (Brains) and 1.90% (Liver), with vital organ mass percentage at 3.25%. The corresponding energy percentages are 7.36% (Kids), 12.81% (Heart), 3.97% (Brain), and 17.10% (Liver), with vital organ energy percentage at 41%. While the brain mass for 70 kg human is predicted as 0.28 kg from allometry, Gallagher's data brain mass is 1.4 kg indicating high EQ. The underprediction of human brain mass and energy percentage is due to the EQ factor, as humans have the highest EQ (i.e., a larger brain size compared to animals of similar mass). This additional brain mass enhances cognitive abilities beyond general brain mass versus body mass scaling laws. See Section 3.4 for further discussion on brain mass and its effects on human results.

b) Organ Mass Based Allometry (OMA) Exponents for SOrMR$_k$ or $\dot{q}_{k,m}$: It is noted that "$f_{k,6}$" in BMA for the vital organs of the six species selected in EAR by Wang et al. [21] are all negative. To explain the negative values of $f_{k,6}$ in BMA for organs, the BMA is replaced by organ mass-based allometry [3], using the relation between organ mass and body mass. Thus,

$$\dot{q}_{k,m} = e_{k,6} M_B^{\,f_{k,6}} = E_{k,6} m_k^{\,F_{k,6}}, \quad f_{k,6} < 0, \quad F_{k,6} < 0, \quad k = Br, H, K, L, R \tag{7}$$

where $F_{k,6} = \left(\dfrac{f_{k,6}}{d_{k,6}} \right), \; E_{k,6} = \left(\dfrac{e_{k,6}}{c_{k,6}^{\,(f_{k,6}/d_{k,6})}} \right)$

See Table 1 for the listing of $E_{k,6}$ and $F_{k,6}$. The $F_{k,6}$ becomes more and more negative for increasing organ masses. Ref. [3] explains the rationale for $F_{k,6}$ vs m_k using the ODM hypothesis. It is apparent from the constant $e_{k,6}$ and $f_{k,6}$, or $E_{k,6}$ and $F_{k,6}$ (Table 1) that different organs consume oxygen at different rates, thus indicating different O_2 profiles. Since the ODM hypothesis is used to predict SOrMR$_k$ and

 doi:10.20944/preprints202503.0386.v1

demonstrate Kleiber's law in the current work, a brief outline of Ref. [3] on ODC and ODM is presented below for the convenience of readers.

B) Group or Oxygen-Deficient Combustion (GC or ODC) in Engineering: The engineering literature models the combustion of dense fuel particle suspension (e.g., coal suspensions fired into a boiler) using a spherical fuel-particle cloud of radius $R_{,FC}$, mass m_{FC} and number density of fuel articles n_{FC}, with its surface exposed to a known oxygen mass fraction at the surface $Y_{O2,FC,s}$ (Figure 1) where FC stands for fuel cloud. Thus, the oxygen concentration, $Y_{O2}(r)$, within the FC is a function of *r*, and consequently, the energy release rate (ERR) varies as a function of *r*, with the highest value near aerobic cloud surface and lowest value at the core of the suspension. This model is referred to as a group combustion or oxygen-deficient combustion (GC or ODC) in engineering literature, implying that particles at the core may not receive enough oxygen to burn. Detailed literature on ODC in engineering is provided in a three-part series of articles [25–27]. The local O_2 consumption rate by each particle located at *r* { $\dot{w}_{O2,p}(r)$ }, is given as (Figure 1d)

$$\dot{w}_{O2,p}(r) = C_{ch,p} Y_{O2}(r), \tag{8}$$

where the characteristic oxygen consumption rate, $C_{ch,p}$, for each particle changes depending on kinetics control ($C_{Ch,p} = C_{Ch,p,kin}$) with a first-order reaction or diffusion control ($C_{Ch,p} = C_{Ch,p,dif}$). The basic relations for $C_{ch,p}$ are given in Ref. [3]. The engineering literature presents the solutions for the i) $Y_{O2}(r)$ profiles within the fuel cloud (FC) and ii) the consumption rate of O_2 by all the particles within the cloud $\dot{w}_{O2,FC}$. The energy release rate (ERR) of FC is given in terms of oxygen consumption by FC { $ERR = \dot{w}_{O2,FC}\ HHV_{O2}$, See Table 1 for HHV_{O2} }. Then, the specific energy release rate of whole cloud , SERRm, is given as ERR/m_{FC}. The SERRm decreases with an increase in $R_{,FC}$ or $m_{,FC}$ – that is, the increase in ERR is less than proportional to the increase in $m_{,FC}$ due to core particles contributing negligible energy release due to OD. The solutions for $\dot{w}_{O2,FC}$, or ERR of FC, are presented in terms of the effectiveness factor ($\eta_{eff,,FC}$) of the FC. The $\eta_{eff,,FC}$ is defined as a ratio of the O_2 consumption rate by all particles within the cloud to the rate of consumption of O_2 in the case that each particle within the FC is subjected to $Y_{O2,FC,s}$.

$$\eta_{eff,FC} = \frac{\dot{w}_{O2,FC}}{\dot{w}_{O2,FC}\left(Y_{O2,FC,s}\right)} \ or\ \frac{\dot{w}_{O2,FC,m}}{\dot{w}_{O2,FC,m}\left(Y_{O2,FC,s}\right)} = \frac{ERR}{ERR\ with\ Y_{O2,FC,s}} \ or\ \frac{SERR}{SERR\ with\ Y_{O2,FC,s}} \tag{9}$$

The solution for $\eta_{eff,FC}$ for a spherical FC is obtained with known $Y_{O2}(r)$ profiles:

$$\eta_{eff,FC} = 3\int_0^1 \left\{\frac{Y_{O2}(r)}{Y_{O2,FC,s}}\right\}\frac{r}{R}\,d\left(\frac{r}{R}\right) = \frac{3}{\sqrt{G}}\left\{\frac{1}{tanh\left(\sqrt{G}\right)} - \frac{1}{\sqrt{G}}\right\},\ Sphere,\ Carbon\ Cloud \tag{10}$$

where the dimensionless group G for FC is defined as:

$$G = \frac{C_{ch,p}\ n_{FC}\ R_{FC}^{\ 2}}{\rho D} = \Psi_T^{\ 2}, \tag{11}$$

and the G number for FC is shown to be related to Thiele Modulus, Ψ_T ($G = \Psi_T^{\ 2}$) in porous char combustion literature [26–28]: Using Equation 10, the effectiveness factor can be plotted against G as shown in Figure 2. It is noted that $G \propto R_{FC}^{\ 2}$, and since the mass of the fuel cloud, $m_{FC} \propto R_{FC}^{\ 3}$ and hence $G \propto m_{FC}^{\ (2/3)}$, assuming a constant number density of fuel particles (n_{FC}).

Figure 2 shows the results for η_{eff} vs. G for a spherical FC. There are three regimes of FC oxidation: Zone I – Dilute Cloud {G<1} where a low number density "n_{FC}" for given FC size R_{FC} or smaller cloud size for given number density "n_{FC}" i.e. "m_{FC}" low) a) indicates high SERR (W/kg). It is

Preprints.org (www.preprints.org) | NOT PEER-REVIEWED | Posted: 5 March 2025 doi:10.20944/preprints202503.0386.v1

constant throughout the cloud since $Y_{O2} = Y_{O2,FC,s}$ and $\eta_{eff,FC} \approx 1$. The particles in Zone I burn almost uniformly with an O_2 concentration at $Y_{O2,FC,s}$ for all particles as though each particle is isolated. Zone II – Dense Cloud {1 < G < 100} , where the cloud size R_{FC} is large, "m_{FC}" is higher, and SERR is a function of *r* since $Y_{O2}(r) < Y_{O2,FC,s}$. This is the ODC mode or "crowd" effect as called in biology [12], where oxygen concentration decreases with decreasing *r*, forming an anaerobic core of radius R_{an} where the O_2 concentration is almost zero. For this zone, $\eta_{eff,FC} < 1$ (Figure 1b). Zone III – Very Dense Cloud {G > 100}, where particles at the core experience severe ODC, with G > 100. (Figure 1c). Except for a thin aerobic film near the surface of FC, the anaerobic core radius is almost the same as R_{FC}. For this zone, $\eta_{eff,FC} << 1$.

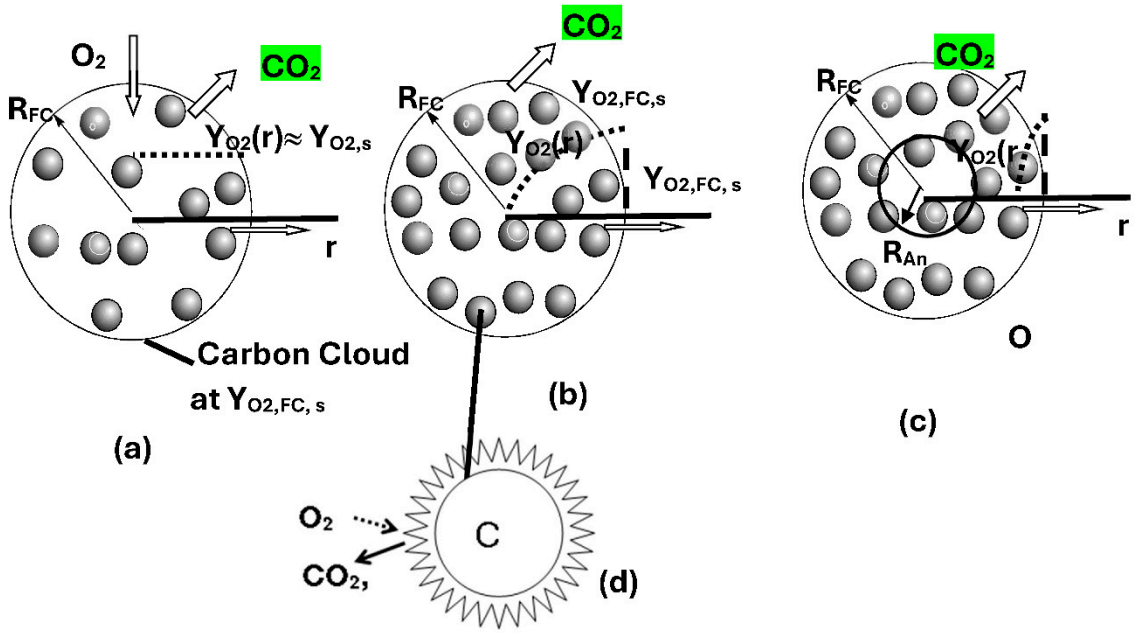

Figure 1. Spherical Fuel/Carbon (FC) Cloud of radius R with fuel particles of diameter d_p and number density n_{FC}, subjected to $Y_{O2,FC,s}$, and temperature T_s at cloud surface. Figure adapted from Ref [3] and modified. **(a)** Dilute Cloud (n is extremely low): Energy release in Isolated Combustion Mode with uniform O_2 concentration at $Y_{O2,FC,s}$. **(b)** Dense Cloud**:** Interactive Combustion Mode with a decreasing O_2 concentration, $Y_{O2}(r)$ within the cloud, resulting in non-uniform O_2 consumption per unit volume. **(c)** Very Dense Cloud: Combustion with an anaerobic core of radius $R_{an,FC}$, where the O_2 concentration is almost zero. **d)** Each particle within the cloud releases energy following either first-order kinetic control or diffusive control, both of which are proportional to the local $Y_{O2}(r)$, $\dot{w}_{O2,p}(r) = C_{ch,p} Y_{O2}(r)$ with $C_{Ch,p}$ as the proportionality constant and relations for $C_{Ch,p}$ in Ref. [3].

C) Oxygen-Deficient Metabolism (ODM) in Biology:

The oxygen diffuses from capillaries towards the metabolic cells contained within interstitial fluid (IF). Even though the biology literature suggests a radial diffusion distance of the order of 100 μm (where $pO_2 \approx 0$) from the capillaries, the actual path may be longer, leading to a decreased O_2 transport rate (or decreased effective diffusivity) to the mitochondria. The diffusive O_2 transport rate is affected due to the following:

$$\dot{q}_{k,m}\left(\frac{W}{kg\ of\ organ\ k}\right) = e_{k,6} M_B^{f_{k,6}} = E_{k,6}\ m_k^{F_{k,6}},\ m_k = c_{k,6}\ M_B^{d_{k,6}};\ F_{k,6} = \left(\frac{f_{k,6}}{d_{k,6}}\right),\quad E_{k,6} = \left\{\frac{e_{k,6}}{c_{k,6}^{\frac{f_{k,6}}{d_{k,6}}}}\right\};\ m_k, M_B\ \ in\ kg$$

 doi:10.20944/preprints202503.0386.v1

If the mass of each kidney (k= Skid, single kidney) is used, $m_{Skid} = m_{Kid}/2$,

$$\dot{q}_{Kid,m}\left(\frac{W}{kg\ of\ organ\ Kid}\right) = e_{k,6}M_B^{f_{k,6}} = E_{k,6}\ m_{Kids}{}^{F_{k,6}} = E_{Skid,6}\ m_{Skid}{}^{F_{k,6}},\ E_{Skid,6} = 2^{F_{k,6}}E_{k,6},\ k = Kid$$

HHV_{O2}= 14,335 kJ/kg of O_2 or 18.7 kJ/SATP L of O_2 or 20.5 J/CST mL of O_2 or 18.1 J/mL of O_2 at 36.2 °C

$HHVO_2$, kJ/L O_2 71 to 92 kg = 15.818 + 5.17* RQ [30–32]: i) closely packed cells (number density of cells, *n*, or crowding effect) [33], ii) tortuous oxygen path, iii) amount of aqueous fluid, iv) extracellular structures or cell barriers, and v) presence of cytoplasm (which alone reduces D by 30 times the normal level). As a result, cells cannot maintain the required O_2 flow for ATP production [34], leading to oxygen deficiency (OD).

Table 1. Allometric Constants for Organ Mass, Energy Release (Metabolic) Rate. Values are based on six species: Rat (0.45 kg), Rabbit (2.5 kg), Cat (3 kg), Dog (10 kg), Human-1 (65 kg), Human-2 (70 kg). (Adopted and modified from Wang–5 organ model, Table 4 of Ref. [29]). The body is composed of four vital organs, BrHKidL, with the fifth organ representing the rest of the mass of the body (RM). Constants $c_{k,6}$, $d_{k,6}$, $e_{k,6}$ and $f_{k,6}$ are from Ref. [21]; density from Ref. [22]).

Organ	ρ_k, g/cc	$c_{k,6}$, [1] kg	$d_{k,6}$[2]	$e_{k,6}$ [3]	$f_{k,6}$ [4]	m_k (85 kg human)	$E_{k,6}$	$F_{k,6}$	$\dot{q}_{k,m}$ (85 kg human)	$c_{k,116}$ [3]	$d_{k,116}$ [3]	OEF_k) 84 kg human)
Kidneys (Kids)[5]	1.05	0.007	0.85	33.41	-0.08	0.31	20.94	-0.094	0.11	0.00631	0.728	0.085
Heart (H)	1.06	0.006	0.98	43.11	-0.12	0.47	23.04	-0.122	0.15	0.00580	0.932	0.48
Brain (Br)	1.036	0.011	0.76	21.62	-0.14	0.32	9.42	-0.184	0.044	0.0108	0.886	0.37
Liver (L)	1.06	0.033	0.87	33.11	-0.27	1.57	11.49	-0.310	0.19	0.0286	0.872	0.52
RM[6]		0.939	1.01	1.45	-0.17	83.44	1.44	-0.168	0.19	0.940	1.007	

ODM in Organs: Hypoxic conditions (low pO_2 in cells) decrease the oxygen consumption rate $\{\dot{w}_{O2}\}_{cell}$ by cells, while anemic conditions or a reduction in blood flow [35] or reduced Hb contents cause a decrease in O_2 supply to the cells from capillaries. Hypoxic conditions cause in reduction of

[1] 50-70 kg Human brains indicate jump in masses from 1.2 kg to 1.4 kg compared to sheep of comparable body mass of 52 kg with m_{Br}= 0.11kg. Human.

[2] Same as footnote (a).

[3] Elia values for "e_k" are [8]: Kids, H, Br, L, SM,AT, RM-ex 2: 21.3, 21.3, 11.62, 9.7, 0.63 , 0.22, 0.58 W/kg [12] and f_k = 0; $m_{RM\text{-}ex2}$ = MB-mvit-m_{SM}-m_{AT}.

Krebs report that the SOrMRk of organs decreases with an increase in body mass, and the order of decrease is the same as the decrease in SBMR of the body [54]. The constants $ck_{,6}$, $dk_{,6}$ etc., are based on data from six species [11] and $ck_{,116}$, $dk_{,116}$ etc., are based on 116 species [14].

Elia constant SOrMRk (W/kg) for Kids, H, Br, L and RM: i.e., ek, 21.3, 21.3, 11.62, 9.7, and 0.58 W/kg and f_k for Elia = 0.

Later et al. [141], for species MB: 70-80 kg, eR: 0.463 W/kg, fR = 0, qR,m = constant, AT mass isometric with body mass [31].

[4]Ref. [41] cites Hepatocytes: f_k = -0.17 to 0.21; kidney cortex: –0.11 to –0.07, brain: –0.07, spleen: –0.14 and lung: –0.10.

For SM based on 49 species, $ck_{,49}$= 0.061, $dk_{,49}$=1.09, M_B from 0.006 to 6600 kg [31].

[5] Gutierrez: kidneys $m_K \propto m_B^{0.85}$; for liver $m_L \propto m_B^{0.87 \text{ to } 0.89}$ [270].

[6] Allometric relation for mass of RM yields different values compared to $m_{RM} = M_B - m_{bital}$ where m_{bital} is based on allometric constants.

 doi:10.20944/preprints202503.0386.v1

ATP production rate leading to "bioenergetic collapse" [36]. Furthermore, Y_{O2} within cells may fall below the "extinction" level, causing cells to cease oxidation and become sleeper cells. OD in cells under hypoxic conditions prevent oxidation of pyruvate and hence it converts to lactate, increasing acidity which then results in the production of protein called HIF (hypoxia-induced factor). HIF enables the ***activity of genes to switch*** from oxidative phosphorylation to glycolytic pathways [37] for energy and ATP release, altering the apparent "software" for energy release from oxidation to glycolysis. ODM promotes a switch to glycolysis, where only two ATP are obtained per CH compared to 32 ATP via oxidative phosphorylation, resulting in the decrease of overall energy release [38] via glycolysis path. Increased ATP requirements cause consumption of more nutrients to adopt an altered metabolic path for energy release, i.e., glycolysis under low-oxygen environments, which supports rapid cell division and serves as a source of energy for cancer cells [39,40]. Rats are known to sustain anoxia for extended periods by using fructose as a nutrient for glycolysis [13,41]. It is well known that oxygen deficiency (OD) or hypoxia contributes to several diseases, including cancer, stroke, anemia and heart disease. There appears to be a positive correlation between the mass of an organ and the number of cancer cases [42], which is attributed to the link between excess fat in organs and obesity.

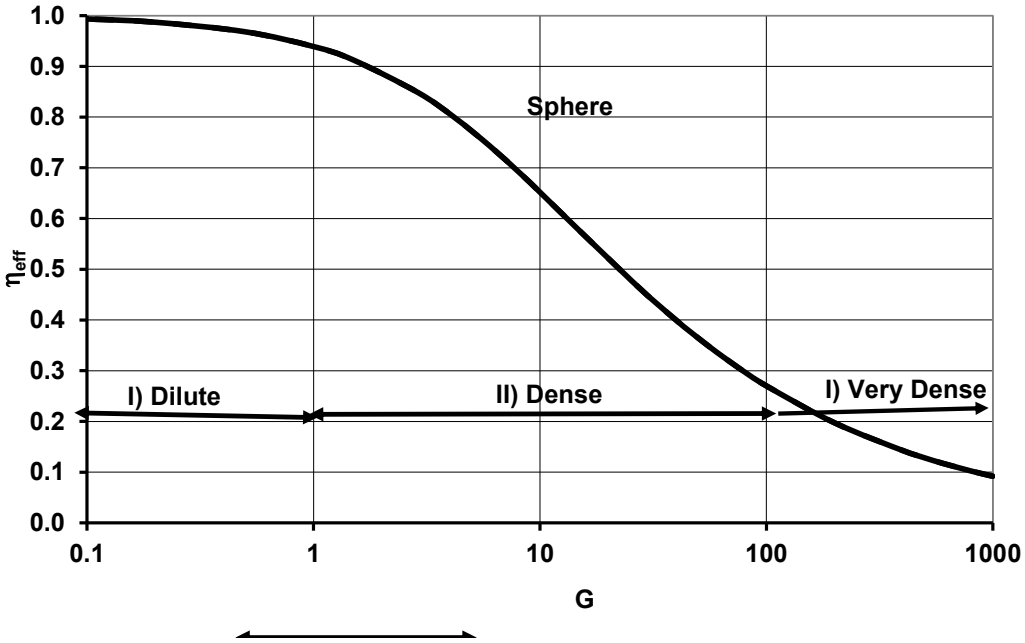

Figure 2. Effectiveness Factor of organ *k* (η_{eff} or $\eta_{eff,k}$ for organ *k* in biology) vs. G (or $G_{OD,k}$ for application to cell clouds in biology). For application to an organ k in a BS, particles are replaced by cells in the ODM model. I) Dilute Cloud: G < 1, within which ηeff ≈ 1, indicating all particles are exposed to the same surface oxygen concentration, or each particle releases energy as though it is isolated. II) Dense Cloud {1 < G < 100: Interactive Combustion Mode or ODC mode with a decreasing oxygen concentration within the cloud, III) Very Dense Cloud: G >100. Particles near the surface oxidize rapidly, while the center of the cloud contains very little oxygen, and particles at the core may not oxidize. The same plot is valid for cell clouds with $\eta_{eff,} = \eta_{eff,k}$, $G = G_{OD,k}$. I) Dilute Cell Cloud: $G_{OD,k} < 1$, within which ηeff ≈ 1, indicating all particles are exposed to same surface oxygen concentration or each cell releases energy as though it is isolated. II) Dense Cell Cloud: Crowding effects of cell or ODM mode with a decreasing oxygen concentration within the cloud, $1 < G_{OD,k} < 100$. III) Very Dense Cloud: $G_{OD,k} > 100$.

ODM in Cell Clouds:

Singer's Phenomenological type of ODM Model: Singer et al. studied the role of OD or the "crowding effect" on the metabolic rates of in-vitro organ samples and developed a

 doi:10.20944/preprints202503.0386.v1

phenomenological type of model. Just like particles in FC, the cells near the aerobic surface undergo high $SOrMR_k$ while those cells near the anerobic core may undergo only glycolysis.

Detailed ODM Model following ODC Literature in Engineering: More detailed ODM models were developed by Annamalai by adapting the ODC literature from engineering to biology [3]. Unlike the Krogh cylinder model, where the capillary is placed on the axis (COA) of a cylinder containing metabolic cells , the ODM model uses a spherical cloud of cells (CC) of radius R_{CC} having n_{CC}, cells per unit volume with capillaries on the surface (COS) of CC with mass of CC, m_{cc} {Figure 3a}. The COS model is also known as the "solid cylinder" model in biology [43]. A detailed comparison between ODC and ODM models, and relations for several variables of interest, are presented in Ref. [3]. In ODM, the carbon cloud is replaced by a cell cloud (CC), particles are replaced by cells of the BS, and $Y_{O2,FC,s}$ becomes $Y_{O2,CC,s}$. The radius R_{FC} is replaced by R_{CC}, the ERR is replaced by the organ metabolic rate (OrMR) and ERR_m is replaced by SOrMR in cell clouds, defined as SOrMR = OrMR / m_{CC}. The G number in engineering ([27]) is also replaced by $G_{OD,k}$ for organ *k*. The oxidation rate for each particle is replaced by the cell metabolic rate (Figure 3d). These relations will be summarized in the methodology section.

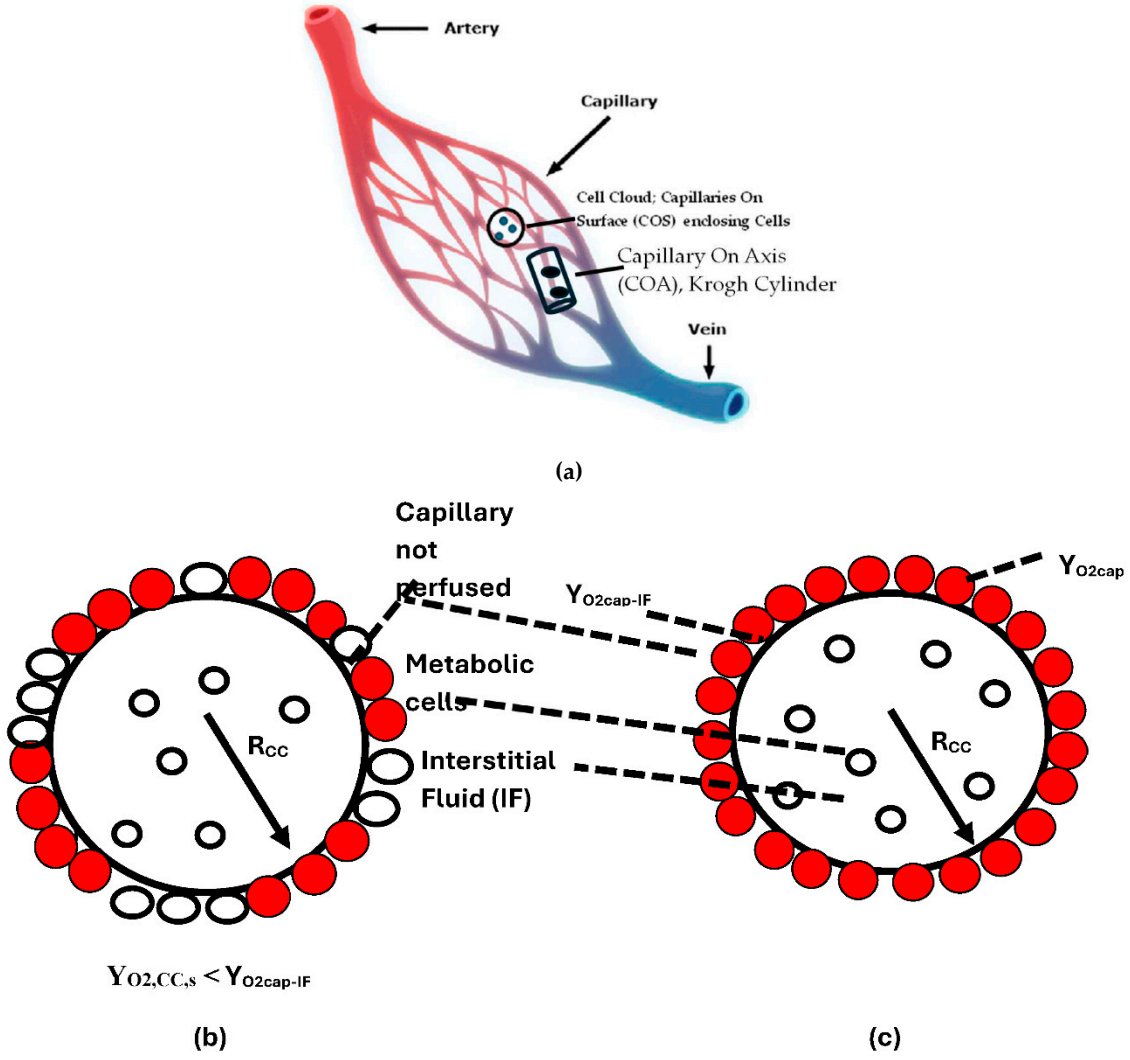

Figure 3. a) Capillary system-Cells can be placed within a cylinder with capillary on axis (COA) or cells can be enclosed by capillaries known as capillary on surface (COS). The (COS) Model is known as the solid "cylinder" model in biology. Figure adopted from [02/27/2025, accessed on https://en.wikipedia.org/wiki/Capillary] and modified. b) COS model for spherical cloud of cells with cell located at "r" consuming O_2 at the rate of $\dot{w}_{O2,cell,k}(r)$; capillaries are partly perfused { e.g Resting condition}. c) COS model with fully perfused

 doi:10.20944/preprints202503.0386.v1

capillaries {e.g exercise} for a spherical cloud of cells. COS model is close to ODC model in engineering literature. The O_2 diffuses towards center of cell cloud (CC) of radius and mass m_{CC}. Cells adjacent to the surface containing capillaries are aerobic, while those farther surface become hypoxic, and the farthest cells are necrotic cells. Detailed results for cell clouds are given in Column 4 of Table 2 in Ref. [3]. Certain regions within organs may undergo only glycolysis due to a lack of O_2. (Adopted from Ref. [3]) with modifications.) Note that for the partly perused capillaries as shown in (b) as in the case of BS under rest, average oxygen mass fraction at the surface of CC , $Y_{O2,CC,s}$ is low. When almost all capillaries are perfused {e.g exercise} as shown in (c) , $Y_{O2,CC,s}$ increases to a maximum.

Just like FC, there exists three zones of operation of CC: Dilute, Dense and very dense CC. More details for CC are provided in the caption of Figure 2. Those cells near the surface are aerobic with higher rate of oxidation of nutrients while those cells near the core of the cloud are anaerobic with very little oxygen. Cells near core may undergo only glycolysis {Figure 3b}.

While resting, limited capillaries are perfused with blood (Figure 3b, surface at $Y_{O22,cc,s}$), whereas under exercise, all the capillaries are perfused (Figure 3c} increasing $Y_{O22,CC,s}$ at the surface of CC { e.g., Maximum Metabolic Rate (MMR) when there is increased blood flow through selected organs during exercise}.

The literature review suggests that despite several hypotheses outlined in Section 1.2 for the 3/4 law, "the hunt for an explanation of the 3/4 law continues" [44]. The current ODM hypothesis focusses on the metabolic rate he controlled by "downstream demand-side" oxygen consumption of all the cells within an organ and provides another "hunt" for an explanation of the 3/4 law. Attempts have also the been made to extend ODM hypothesis predict the allometric constants of maximal metabolic rate (MMR) vs. body mass using known data on the percentage of blood perfused under rest and during exercise, attributing the increase in MR to enhanced oxygen concentration under the redistribution of perfusion percentage of capillaries.

1.3. Objectives

The overall objectives of the current work are to i) link the field of group or oxygen-deficient combustion (ODC) in engineering with the field of oxygen-deficient metabolism (ODM) in biology, ii) adopt the relations developed for energy release rate per unit mass (ERR_m, W/kg cloud) to predict SOrMRk (W/kg of k) of 116 BS ranging in mass from 0.0075 to 6,650 kg using known data from two BS, referred to as Reference Species (RS), where RS-1 has the lowest body mass, $M_{B,RS-1}$ (Shrew, 0.0075 kg), and RS-2 has m_{RS-2} body mass much higher than m_{RS-1} (Rat Wistar of 0.390 kg, $\eta_{eff,k} < 1$), and iii) estimate the whole-body metabolic rate versus M_B using a heterogeneous approach and known organ masses, demonstrating Kleiber's law with an exponent close to 0.75. In addition, predict a) a hypothetical upper metabolic rate (UMR) for organs, and, consequently, the whole body in the case all the cells within the organ metabolize without the presence of oxygen concentration gradients, b) the maximal metabolic rate (MMR) under exercise, when all the capillaries at the cell cloud surface are perfused, with increased average oxygen concentration at the cell cloud surface (CC,s) and show that whole-body allometric law yields an exponent close to 0.87, as quoted in the literature, and c) provide a method for detecting the degree of oxygen deficiency within organs for medical personnel.

2. Materials and Methods

2.1. ODM Hypothesis

The ODM hypothesis assumes that each organ *k* consists of multiple cell clouds (CC), with each cell cloud having a mass mass $m_{cc,k}$ with radius $R_{CC,k}$, which is related to the organ mass m_k by $R_{CC,k}$ α $m_k^{1/3}$. It is also possible that capillaries do not fully cover the entire spherical surface enclosing the cells (Figure 3). Typically, 25-35 % of an organ's capillaries are perfused at rest, with perfusion increasing during exercise since there is increased metabolic demand and a higher perfusion percentage results in a higher $Y_{O2,cc,s}$. Using the Krogh-Erlang equation, Ostergaad demonstrated that

 doi:10.20944/preprints202503.0386.v1

only 10% of SM capillaries are perfused at rest, but more capillaries are recruited during exercise [46]. Further details can be found in Section 2.2 and Section 3.4.

Smaller species have smaller organs (e.g., shrew of mass 0.0075 kg), while larger species have larger organs, as indicated by $d_k > 0$ in the allometric exponents for organ sizes. Thus, the smaller organs of smaller species may have shorter distances for O_2 diffusion from capillaries to cells, allowing metabolism to occur as if each cell within the CC is exposed to the same O_2 concentration as $Y_{O2,CC,s}$ ($\eta_{eff} \approx 1$), resulting in $SOrMR_k \approx SOrMR_{k,iso,}$. However, isolated cell metabolic rates can still vary from organ to organ, even in smaller species, due to differences in functional requirements, cell reactivity, and O_2 transport rate (e.g., heart tissues containing M_b can deliver O_2 at faster rate resulting in increased effective transport coefficients for O_2 from capillaries to mitochondria). As organ mass increases (e.g., in the liver), $\eta_{eff,k} < 1$, and $SOrMR_k \approx \eta_{eff,k} \times SOrMR_{k,iso,}$ where it is assumed that for any given organ *k*, $SOrMR_{k,iso}$ remains constant for all BS regardless of body size, but becomes extremely low for larger organs in larger species, leading to lower values of $\eta_{eff,k}$.

2.2. Methodology

Detailed comparisons of the governing conservation equations and several relations in the fields of ODC in engineering and ODM in biology literatures are presented in Ref. [3]. These include: i) conservation equations for both fields, ii) the ERR of a single particle in a FC and a single cell in a CC in terms of Y_{O2}, iii) oxygen profiles in FC versus CC, iv) the dimensionless G number for FC {Equation 118 } and corresponding $G_{OD,k}$ for the CC of organ *k* in biology { Equation 14} and v) the specific ERR (SERR) of FC (W/kg of cloud) in terms of the effectiveness factor and G, and specific organ metabolic rate ($SOrMR_k$) of CC (W/kg of cell cloud of organ *k*) in terms of the effectiveness factor and $G_{OD,k}$. The relevant relations for the current work are briefly summarized below.

i) Metabolic Rate of single cell located at r in CC {Figure 3}

$$\dot{w}_{O2,cell,k}(r) = \left(C_{ch,cell}\right)_k \; Y_{O2}(r), \tag{12}$$

where $C_{Ch,cell}$, characteristic cell O_2 consumption rate when $Y_{O2} = 1$; the relations for $C_{Ch,cell}$ under kinetic control or diffusion controlled O_2 consumption rates are given in Ref. [3].

ii) Oxygen Profiles within CC

For the cell cloud within organ *k*, Ref. [3] presents

$$\frac{Y_{O2,k}(\xi)}{\left(Y_{O2,k}\right)_{\xi=1}} = \frac{Y_{O2,k}(\xi)}{\left(Y_{O2,CC,s}\right)} = \left(\frac{1}{\xi}\right)\frac{Sinh\left(G_{OD,k}{}^{1/2}\xi\right)}{Sinh\left(G_{OD,k}{}^{1/2}\right)}, \quad \xi = \left(\frac{r}{R_{CC,k}}\right) \tag{13}$$

where for organ k

$$G_{OD,k} = \frac{\left(C_{ch,cell}\right)_k n_k R_{CC,k}{}^2}{\rho D} = \frac{Characteristic\ O_2 consumption\ rate\ by\ cell\ cloud}{Characteristic\ O_2 transport\ rate\ to\ cells\ from\ cell\ cloud\ surface} \tag{14}$$

where *k*= Kid, H, Br, L and $R_{CC,k} \propto m_k^{1/3}$, $C_{Ch,cell,}$ characteristic O2 consumption rate by cell

iii) Effectiveness Factor of Spherical CC and Specific Organ Metabolic Rate {$SOrMR_k$}

Adopting the same procedure as in engineering,

$$\eta_{eff,k} = \frac{\dot{w}_{O2,m,k}}{\dot{w}_{O2,m,k}\left(Y_{O2,CC,s}\right)} = \frac{\{SOrMR\}_k}{\left\{SOrMR\left(Y_{O2,CC,s}\right)\right\}_k} = 3\int_0^1 \left\{\frac{Y_{O2,k}(r)}{\left(Y_{O2,CC,s}\right)_k}\right\}\frac{r}{R_{CC,k}}\,d\left(\frac{r}{R_{CC,k}}\right), \; Spherical\ CC \tag{15}$$

With Y_{O2} profile from Equation 13, the $\eta_{eff,k}$ is derived as:

 doi:10.20944/preprints202503.0386.v1

$$\eta_{eff,k} = \frac{\{SOrMR\}_k}{\{SOrMR(Y_{O2,CC,s})\}_k} = \frac{3}{\sqrt{G_{OD,k}}}\left\{\frac{1}{tanh\left(\sqrt{G_{OD,k}}\right)} - \frac{1}{\sqrt{G_{OD,k}}}\right\},\ Spherical\ CC \quad (16)$$

where k = Kids, H, Br, and L Using the definition of $\eta_{eff,k}$, the SOrMR$_k$ is given as

$$\{SOrMR\}_k = \eta_{eff,k}\ \ \{SOrMR(Y_{O2,CC,s})\}_k = \eta_{eff,k}\ \dot{q}_{k,m,iso} \quad (17)$$

where $\dot{q}_{k,m,iso} = \{SOrMR(Y_{O2,CC,s})\}_k$. Equation 17 reveals that SOrMR$_k$ is a function of G$_{OD,k}$ in biology due to dependence of $\eta_{eff,k}$ on G$_{OD,k}$. I) When G$_{OD,k}$ << 1 (dilute cloud), then, $\eta_{eff,k} \rightarrow 1$ (Equation 1613, Figure 2 with $\eta_{eff} = \eta_{eff,k}$, G = G$_{OD,k}$). II) As the organ size increases, G$_{OD,k}$ also increases, and the effectiveness factor decreases (dense cloud, 1 < G$_{OD,k}$ < 100). III) When G$_{OD,k}$ > 100, the cell cloud is very dense. All three regimes of $\eta_{eff,k}$ of CC within an organ are shown in Figure 2.

iv) <u>Metabolic Rate of Vital Organs</u> { $\dot{q}_{vit}$ }: Using Equation 17 for the vital organs, the metabolic rates of vital organs of any BS:

$$\dot{q}_{vit} = \eta_{eff,Kid}\ \dot{q}_{Kid,m,iso}\ m_{Kids} + \eta_{eff,H}\ \dot{q}_{H,m,iso}\ m_H + \eta_{eff,Br}\ \dot{q}_{Br,m,,iso} m_{Br} + \eta_{eff,L}\ \dot{q}_{L,m,,iso}\ m_L \quad (18)$$

v) Metabolic Rate of Remaining Mass (RM) of Tissues { $\dot{q}_{RM}$ } for any BS

The remaining mass of organs (RM) represents a sum of all "minor" organs (e.g., SM, skin, etc.) within the body, and the specific metabolic rate of RM (W/kg of RM) is needed. There are several possible approaches: a) Select data for each of minor organ if available, estimate the effectiveness factor for all minor organs, and adopt a similar procedure outlined for vital organs , b) Use the EAR for RM: $\dot{q}_{RM,m} = e_{RM,6}\ M_B^{\ f_{RM,6}}$, e$_{RM,6}$ =1.45, f$_{RM,6}$ = -0.17, $\dot{q}_{RM,m}$ in W/kg, c) Assume Elia's constant values for $\dot{q}_{RM,m}$ as 0.581 W/kg for all BS. In the current work, methods (b) and (c) are adopted for estimating $\dot{q}_{RM,m}$.

$$\dot{q}_{RM} = \dot{q}_{RM,m}\ m_{RM}\ ,\ m_{RM} = M_B - m_{vit} \quad (19)$$

vi) Whole Body Metabolic Rate ($\dot{q}_B$) under Rest

The effective area for O_2 exchange.is limited, as only 25% to 35% of available capillaries are perfused under BMR conditions [45], which affects O_2 diffusion distance and hence the metabolic rate within the organ. Adopting the heterogeneous method, whole body metabolic rate under rest, { $\dot{q}_B$ } is given as

$$\dot{q}_B = \dot{q}_{vit} + \dot{q}_{RM} = \eta_{eff,Kids}\ \dot{q}_{Kid,m,iso}\ m_{Kids} + \eta_{eff,H}\ \dot{q}_{H,m,iso}\ m_H + \eta_{eff,H}\ \dot{q}_{Br,m,,iso} m_{Br} + \eta_{eff,L}\ \dot{q}_{L,m,,iso}\ m_L + \dot{q}_{RM,m}\ m_{RM} \quad (20)$$

vii) Metabolic Rate of RM { $\dot{q}_{RM,Ex}$ } and Whole Body Metabolic Rate { $\dot{q}_{B,Ex}$ } under Exercise

 doi:10.20944/preprints202503.0386.v1

During exercise, blood flow to the skeletal muscle (SM) is increased to supply the required oxygen and nutrients. Thus, SM becomes metabolically more active compared to other tissues within the RM due to increased capillary perfusion, increasing from approximately 25% at rest to nearly 90 % during exercise.

$$\dot{q}_{SM} = \dot{q}_{SM,m} \quad m_{SM} \tag{21}$$

Relations for $\dot{q}_{SM,m}$ depends upon the $Y_{O2,CC,s}$ and hence the percentage of capillaries perfused. The remaining mass of tissues under exercise is given as $m_{RM,Ex} = M_B - m_{vit} - m_{SM}$

$$\dot{q}_{B,Ex} = \dot{q}_{vit,Ex} + \dot{q}_{SM} + \dot{q}_{RM-Ex} \tag{22}$$

Where $\dot{q}_{vit,Ex}$ is different from $\dot{q}_{vit}$ under rest due to the percentage of capillaries perfused under exercise are different from those at rest. The $\dot{q}_{RM,Ex}$ during exercise is given as,

$$\dot{q}_{RM,Ex} = \dot{q}_{RM,Ex,m} \quad m_{RM,Ex}\ ,\ m_{RM,Ex} = M_B - m_{vit} - m_{SM} \tag{23}$$

viii) Upper Metabolic Rate (UPR, $\dot{q}_{B,UPR}$) and Maximum Metabolic Rate (MMR, $\dot{q}_{B,MMR}$) of Whole Body

A hypothetical upper MR of organ *k* (not the maximum MR) and, hence, the whole-body MR can be estimated by setting $\eta_{eff,k} = 1$ for all organs {i.e. no oxygen gradients within CC}, including RM from Equation 1613 to Equation 2016.

When the CC surface is covered with more perfused capillaries, the $Y_{O2,CC,s}$ increases and most of the cells are aerobic resulting in the maximum metabolic rate, MMR and leading to a whole-body allometric law with an exponent higher than 0.75. The MMR, such as during exercise, is obtained by setting $\eta_{eff,k} = 1$ for all organs, including SM, and RM-Ex during exercise, while adjusting the percentage of capillaries perfused. Further blood flow to organs other than SM are also altered. This adjustment affects $Y_{O2,CC,s}$ for all organs due to change in blood flow rates . The percentage of perfusion affects $Y_{O2,CC,s}$ (Figure 3b and Figure 3c). The change in $Y_{O2,CC,s}$ is given by the following relation:

$$\frac{\left(Y_{O2,CC,s}\right)_{k,MMR}}{\left(Y_{O2,CC,s}\right)_{k,rest}} = \frac{Blood\ flow\ rate\ to\ organ\ k\ under\ MMR}{Blood\ flow\ rate\ to\ organ\ k\ under\ Rest} \tag{24}$$

The increased $Y_{O2,CC,s}$ causes isolated rates to increase, thereby increasing the whole-body metabolic rate. The percentage of capillaries perfused under rest and exercise conditions is shown in . Note that blood flow rate to organ k is given by the product of blood flow fraction to organ k and the pumping rate of blood by the heart and pumping rate changes depending upon the rest or exercise conditions.

Table 2. Capillary Perfusion Percentage Assumed for MMR. Note: Capillary perfusion percentage does not affect SOrMRk and BMR estimations; they affect only $Y_{O2,CC,s}$ or MMR under exercise. Accessed 02182025 https://courses.lumenlearning.com/suny-ap2/chapter/homeostatic-regulation-of-the-vascular-system/.

Organ	Rest (mL/min)	Mild Exer(mL/min)	Maximal (mL/min)	Rest %	Exercise %	EX-Rest ratios
Kidney	1100	900	600	19	3	0.55
Heart	250	350	750	4	4	3
Brain	750	750	750	13	4	1

 doi:10.20944/preprints202503.0386.v1

Others (i.e., liver, spleen)	600	400	400	10	2	0.67
Skeletal muscle	1200	4500	12500	21	71	10.42
RM-Ex (GI+skin+others)	2500	3000	2900	43	17	1.16

2.3. Estimation of OD Number ($G_{OD,k}$) and Effectiveness Factor ($\eta_{eff,k}$) of Organ k any BS

The estimation of $\eta_{eff,k}$ requires knowledge of the dimensionless number $G_{OD,k}$ (Equation 14), which depends on i) the reactivity of cells within organ *k* undergoing metabolism ($C_{Ch,cell}$) either under diffusion or kinetic control { Michaelis Menten (MM) constant for first order reaction under adsorption control} ii) the overall transport coefficient *D* of oxygen from capillaries to mitochondria, and iii) a knowledge of $(Y_{O2,CC,s})_k$ dictated by capillary number density and percentage of capillaries perfused. There are two methods for estimating $SOrMR_k$ of organs:

A) Basic Method: This approach requires basic data for $C_{Ch,cell}$, D, $(Y_{O2,CC,s})_k$, MM constant and the percentage of capillaries perfused for each organ *k*. Consequently, greater uncertainty exists in the estimation of $G_{OD,k}$ and $SOrMR_k$ due to variations in these parameters across the organs of 116 species.

B) Ratio Method or Reference Species (RS) Method:

The current work uses the references species (RS) method, also known as the ratio method, and assumes that the $SOrMR_k$ of two references species, RS-1 and RS-2, are known. This approach reduces uncertainty in the results by relying on ratios. This method is based on the premise thats $\dot{q}_{k,m,iso}$ of any BS is same as $\dot{q}_{k,m}$ of RS-1 having lowest body mass and hence lowest organ mass. In RS-1, all cells within the vital organ *k* operate under an isolated mode (i.e., all cells at $Y_{O2,CC,s}$, $\eta_{eff,k} \approx 1$). The RS-1 is selected as the BS with the lowest body mass (e.g., RS-1: Shrew, 7.6 g). Justification is as follows. Makarieva et al. [47] demonstrated that SBMR varied from 0.3 W/kg to 9 W/kg (a 25-fold variation), despite a 10^{20}-fold difference in body mass for "bacteria to elephants and algae to trees." This suggests that SBMR is relatively consistent among mammalian species [48]. Since the number of cells per unit mass is similar across BS, then cell metabolic rate (CMR) does not vary significantly. This view is confirmed by Lindstedt and Schafeer [49], who stated that the "150-ton blue whale," which is 75 million times the mass of the 2g Etruscan shrew, "shares the same architecture… organ systems, biochemical pathways." Therefore, the isolated metabolic rate of cells in a vital organ *k* of any BS is assumed to be same as that of organ *k* of RS-1.

The RS-2 is selected as a BS with a significantly higher body mass (e.g., Rat Wistar, 390 g) than RS-1. In RS-2, the $G_{OD,k}$ falls within the dense zone (i.e., the steeper part of $\eta_{eff,k}$ vs. $G_{OD,k}$, Zone II in Figure 2), and hence $(\eta_{eff,k})_{RS\text{-}2} < 1$. With the known $SOrM_k$ data for RS-1 and RS-2, $(\eta_{eff,k})_{RS\text{-}2}$ is estimated as

$$\left\{\eta_{eff,k}\right\}_{RS-2} = \frac{\left(SOrMR_{k,RS-2}\right)}{\left(SOrMR_{k,iso,RS-2}\right)} \approx \frac{\left(SOrMR_{k,RS-2}\right)}{\left(SOrMR_{k,RS-1}\right)} \tag{25}$$

and the corresponding $(G_{OD,k})_{RS\text{-}2}$ is evaluated using Equation 1613. With the assumption of a constant cell diameter (2a) for a given organ *k* across BS (Schmidt-Nielsen [58], Savage et al. [49]) and the number density of cells, and using the definition of $G_{OD,k}$ (Equation 14), $G_{OD,k} \propto R_{CC,k}^{\ 2}$ and since the mass of the cell cloud, $m_{CC,k} \propto R_{CC,k}^{\ 1/3}$, $G_{OD,k} \propto m_{CC,k}^{\ 2/3}$, the $G_{OD,k}$ for 116 other BS (other than RS-1 and RS-2) with body masses ranging from 0.010 kg to 6,650 kg are estimated using the following relation:

$$\frac{\left(G_{OD,k}\right)_{BS}}{\left(G_{OD,k}\right)_{RS-2}} = \left(\frac{m_{k,BS}}{m_{k,RS-2}}\right)^{(2/3)} \tag{26}$$

 doi:10.20944/preprints202503.0386.v1

and the corresponding $\eta_{eff,k}$ is estimated using Equation 1613. Thus, the $SOrMR_k$ for k = Kids, H, Br and L, $\dot{q}_{vit}$ is determined from Equation 1814, $\dot{q}_{RM,m}$, using Equation 1915, where $SOrMR_{RM}$ ($\dot{q}_{RM,m}$) of the RM, which consists of several organs with metabolically weak cells, is estimated by following EAR (Table 1, [21]) since organ masses are not known with remainder tissue mass or using Elia's constant for $SOrMR_{RM}$ (Table 1), and finally, $\dot{q}_B$ can be estimated from Equation 2016, based on the organ masses of 116 species. Results are presented in the next section. A step-by-step procedure is presented in Appendix B and is briefly described here.

3. Results and Discussion

3.1. Whole Body Metabolic Rate using EAR for All Organs and the Effect of Elia's Constant for $\dot{q}_{RM,m}$ on Whole-Body Allometry

A. Empirical Allometric Relations (EAR) for all Organs: Hereafter, Wang's allometric relations will be referred to as EAR (Equation 4) or, $\dot{q}_{k,m} = e_k \; M_B^{\,f_k}$, which are obtained with data on $SOrMR_k$ ($\dot{q}_{k,m}$, W/kg of k, k=Kids, H, Br, L and RM) vers us the body mass for six species. The same allometric constants were then extended to estimate SOrMRk of 116 species, summing up $OrMR_k$ to obtain the whole-body metabolic rate and validating Wang's approach by demonstrating Kleiber's law with a = 3.22 and b = 0.76. Note that EAR is used only for $\dot{q}_{k,m}$ and $\dot{q}_k$ is estimated using organ masses listed in Table 3 { Appendix A} which tabulates the BS, body mass, organ masses for 116 species, and $\dot{q}_B$ using EAR.

B. EAR for Vital Organs and Elia Constant for RM: The author used the same allometric constants for vital organs but assumed Elia's constant q_{RM} of 0.581 W/kg and computed the whole-body metabolic rate. With Elia's constant, $\dot{q}_{RM,m}$, the Kleiber's law exponents become a = 2.49, and b = 0.78. It is seen from Figure 4 that the slope b increased from 0.76 to 0.78, representing a 3.3 % increase in the exponent b when Elis's constant is used for RM.

3.2. Whole Body Metabolic Rate Using ODM Hypothesis and Comparison with Results from EAR Method

A). ODM and EAR for $SOrMR_k$ of RM: The ODM model uses the relation for effectiveness factor of four vital organs to predict $SOrMR_k$ and then whole body metabolic rate using summation over all organs. Figure 5 shows the results for the metabolic rate vs. body mass obtained using ODM hypothesis and using allometric law for $\dot{q}_{RM,m}$ since RM consists we did not carry this fir RM since it has multiple organs of widely varying organ masses with wide variation in allometric exponent "f_k" . Thus Used EAR for " RM" of several metabolically weaker organs .

$$\dot{q}_B(W) = a \; M_B^{\;b} \quad , a=3.04,\ b=0.75,\ M_B = 0.0075\ kg \text{ to } 6650 \tag{27}$$

The same figure provides a comparison with Wang's results using EAR. Note that the ODM method relies only on data from two reference species, RS-1 and RS-2, to predict $SOrMR_k$ and whole-

 doi:10.20944/preprints202503.0386.v1

body metabolic rates for the remaining 114 species. Table 3 compares ODM based metabolic rate $\dot{q}_B$ for 116 species with those $\dot{q}_B$ using EAR (last 2 columns).

If the error percentage is defined as {MR with ODM - MR with EAR) * 100 } / {MR with EAR } , then the highest error occurs for a 60 kg human at 24.07%. The average error across 116 species is 8.14%.

B). ODM and Elia's Constant SOrMRk for RM: Instead of using the allometric relation for SOrMRk of RM, if Elia's consonant value for RM ($\dot{q}_{RM,m} = 0.581$ W/kg) is applied, the allometric constant *b* increases from 0.75 to 0.77 (Figure 6). When Elia's constant value for is used instead of EAR for RM, lower values re obtained for smaller species but, while higher $\dot{q}_B$ values are observed for larger species, resulting in a 3.3% increase in the slope of *b*.

i) If MR of residual mass (RM), $\dot{q}_{RM,m} = a_{RM}\ M_B^{\ b_{RM}}$, $a_{RM} = 1.45$, $b_{RM} = -0.17$, then for the whole body, a = 3.2162, b = 0.756,

ii) If $\dot{q}_{RM,m} = 0.581$ W/kg {Elia's constant value} of then a = 2.486, b = 0.781.

This increase in *b* is nearly the same as in the EAR method. The residual mass (non-vital mass) seems to play a minor role in determining the exponent *b*, since the vital organs are more metabolically [40] active. The current ODM method for SOrMRk is validated, as it supports Kleiber's law using data from only two BS (Figure 5).

When the EAR method for SOrMR is used [21], the whole-body specific metabolic rate for a 60 kg human is 1.51 W/kg and 1.41 W/kg for a 70 kg human. In contrast, the current ODM estimates 1.144 W/kg for a 60 kg human and 1.108 W/kg for a 70 kg human. Holliday et al. (1967) reported an observed value of 1.21 W/kg [50]. Thus, the results from the ODM method align more closely with the literature data on humans.

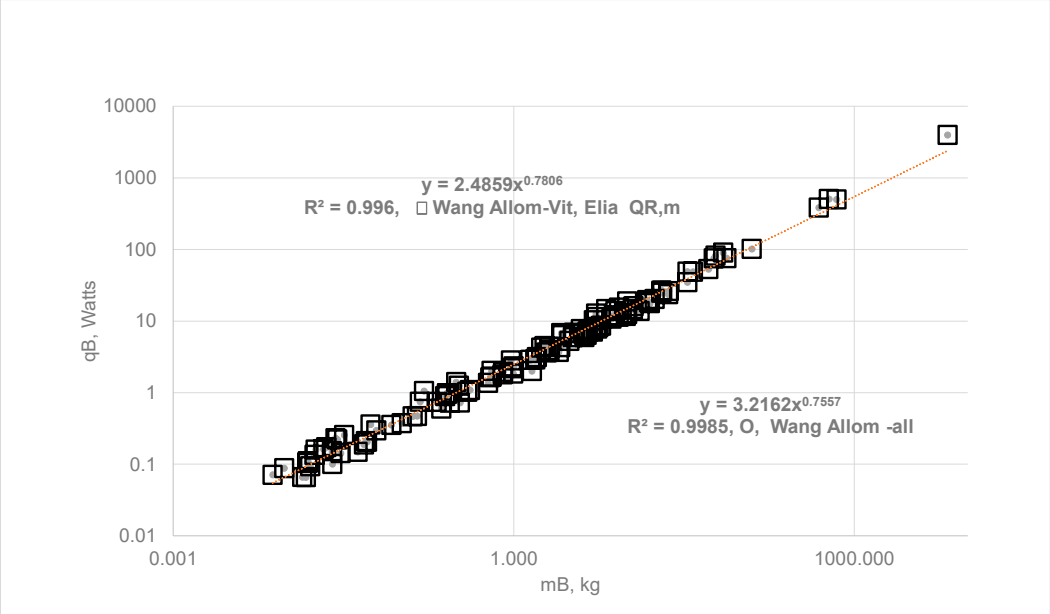

Figure 4. The constants in SOrMRk relations were based on data from organ metabolic rates of six species ranging in mass from 0.48 kg to 70 kg. Whole-body metabolic rates of 116 species (ranging from 0.0076 to 6,650 kg), for which organ masses are known, were obtained by assuming the SOrMRk values derived from the six species are valid for the organs of all 116 species. Using these data and the known organ mases of the 116 species, whole-body metabolic rates were estimated for BS with body mass ranging from 0.0075 kg to 6,650 [21]. .

Preprints.org (www.preprints.org) | NOT PEER-REVIEWED | Posted: 5 March 2025 doi:10.20944/preprints202503.0386.v1

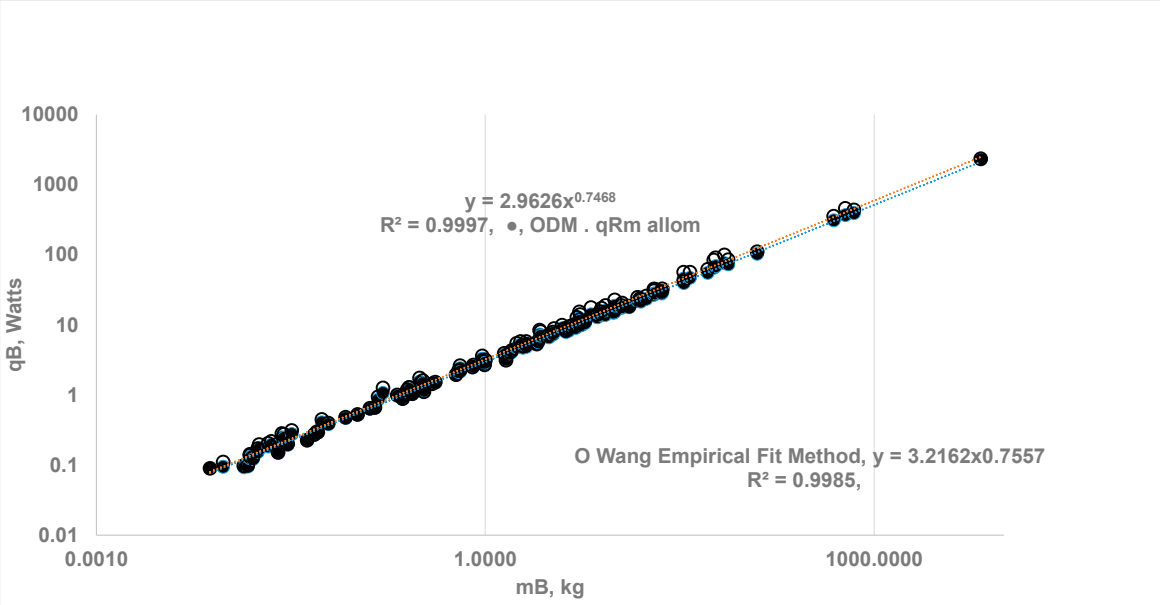

Figure 5. Comparison of whole-body metabolic rate using the ODM Method (with RS-1 = 0.0076 kg RS-2 = 0. 390 kg and EAR for the organs; $\dot{q}_B = a\, M_B^{\ b}$, M_B = 0.0075 kg to 6,650) i) (●) ODM Method: a = 2.963, b = 0.747, ii) (O) EAR Method: a = 3.216, b = 0.756. Kleiber's law constants are almost the same with both methods.

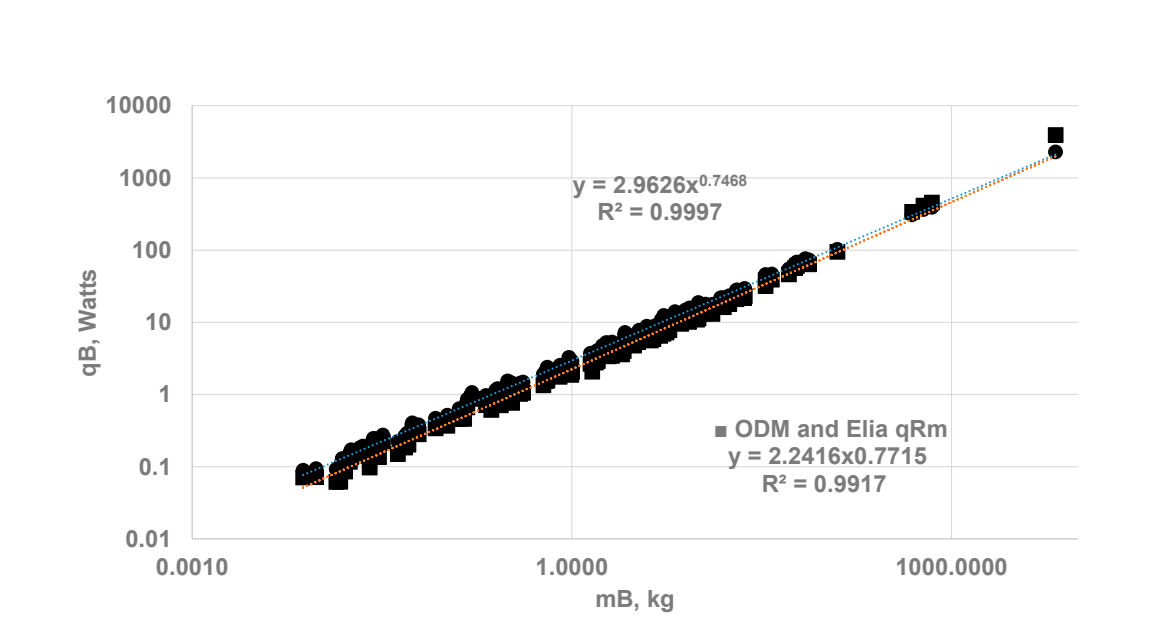

Figure 6. Comparison of ODM based whole-body MR with EAR based MR for BS ranging in mass from 0.0075 to 6,650 kg. Kleiber's law: $\dot{q}_B = a\, M_B^{\ b}$ i) $\dot{q}_{RM,m}$ from the allometric relation: a= 2.963 b= 0.747, ii) $\dot{q}_{RM,m}$ with Elia's constant of 0.581 W/kg, a = 2.242, b = 0.772. The percentage increase in *b* for the ODM method is the same as the percentage increase in the EAR method when $\dot{q}_{RM,m}$ is changed from an allometric law to a constant value for 116 species.

3.3. Vital Organ Contribution Percentage via ODM and Comparison of results with Empirical Allometric Laws

As a further validation of the ODM method, the predicted percentage contribution of vital organs is compared with literature data. Figure 7 shows the computed ERR from the four vital organs versus m_{vit}, while Figure 8 compares the percentage energy contribution of vital organs estimated

Preprints.org (www.preprints.org) | NOT PEER-REVIEWED | Posted: 5 March 2025 doi:10.20944/preprints202503.0386.v1

using ODM with those obtained using EAR. If the allometric fit for $\dot{q}_{vit}$ is expressed as $\dot{q}_{vit} = \alpha_{vit} m_{vit}^{\beta vit}$ with $\dot{q}_{vital}$ in watts, m_{vit} in kg and vital energy contribution as $\%\, vit = \gamma_{vit} M_B^{\nu_{vit}}$, the fits yield α_{vital} = 12.69, β_{vital} = 0.74, γ_{vit} = 51.85, ν_{vil} = -0.115, while previous literature with EAR method for all vital organs suggests α_{vit} = 15.67, β_{vit} = 0.77. γ_{vit} = 49.67 and ν_{vil} = -0.101 [21]. The energy contribution estimated from ODM appears to agree with data from the EAR method for M_B up to 500 kg. The OD in organs results in a slope of $\dot{q}_{vit}$ vs. m_{vit} that is less than 1.

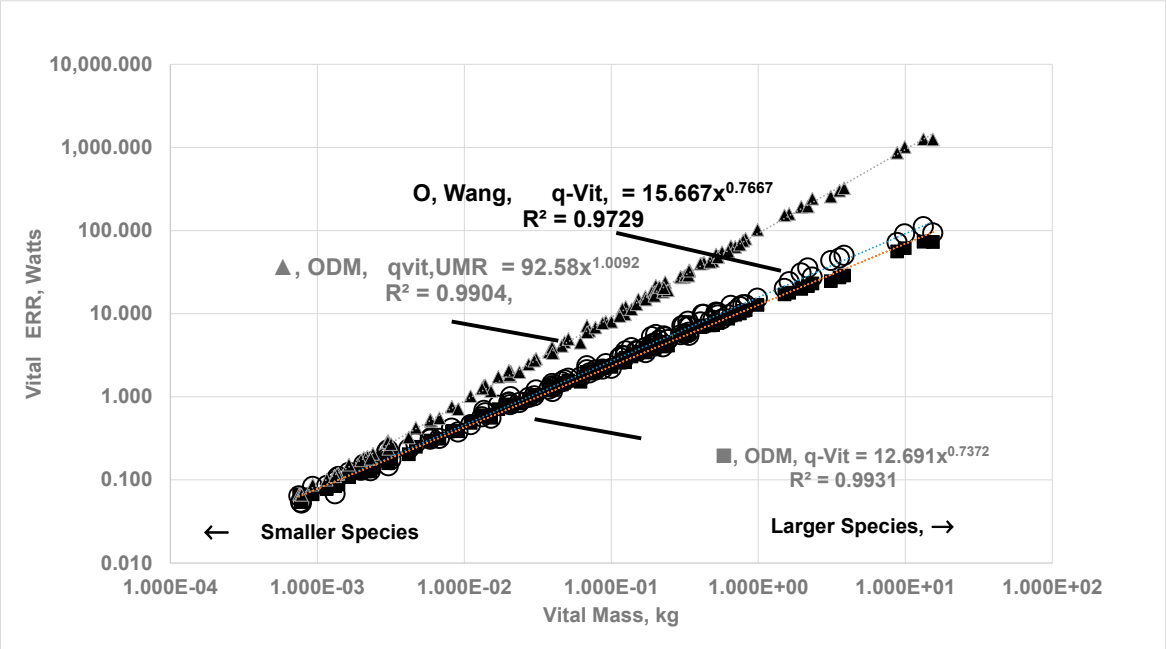

Figure 7. ERR from vital organs and upper ERR ($\eta_{eff,k}$ = 1 for vital organs) as a function of vital organ mass, m_{vit}: Comparison between ODM and EAR data. Vital organ MR (ODM) for 116 with body mass ranging from 0.0076 kg to 6,650 kg; $\dot{q}_{vit} = \alpha_{vit} m_{vit}^{\beta vit}$, $\dot{q}_{vit}$ in watts, m_{vit} in kg. i) (■) ODM Method: α_{vit} = 12.961, β_{vit} = 0.737, ii) (O) EAR Method: α_{vit} = 15.667, β_{vit} = 0.767. $\dot{q}_{vit}$ under ODM are slightly lower compared to $\dot{q}_{vit}$ of EAR. iii) $\dot{q}_{vit.UMR}$ in watts when O_2 gradients disappear for all vital organs ($\eta_{eff,k}$ = 1 when $\eta_{eff,k}$ = 1 for all vital organs) (▲): $\dot{q}_{vit,UMR} = \alpha_{vit,UMR} m_{vit}^{\beta vit,UMR}$, $\alpha_{vit,UMR}$ = 92.58, $\beta_{vit,UMR}$ = 1.009. For $\dot{q}_{vit.UMR}$, the law is almost isometric with respect to vital organ mass since all cells in vital organs are exposed to uniform cloud surface oxygen concentration.

Preprints.org (www.preprints.org) | NOT PEER-REVIEWED | Posted: 5 March 2025 doi:10.20944/preprints202503.0386.v1

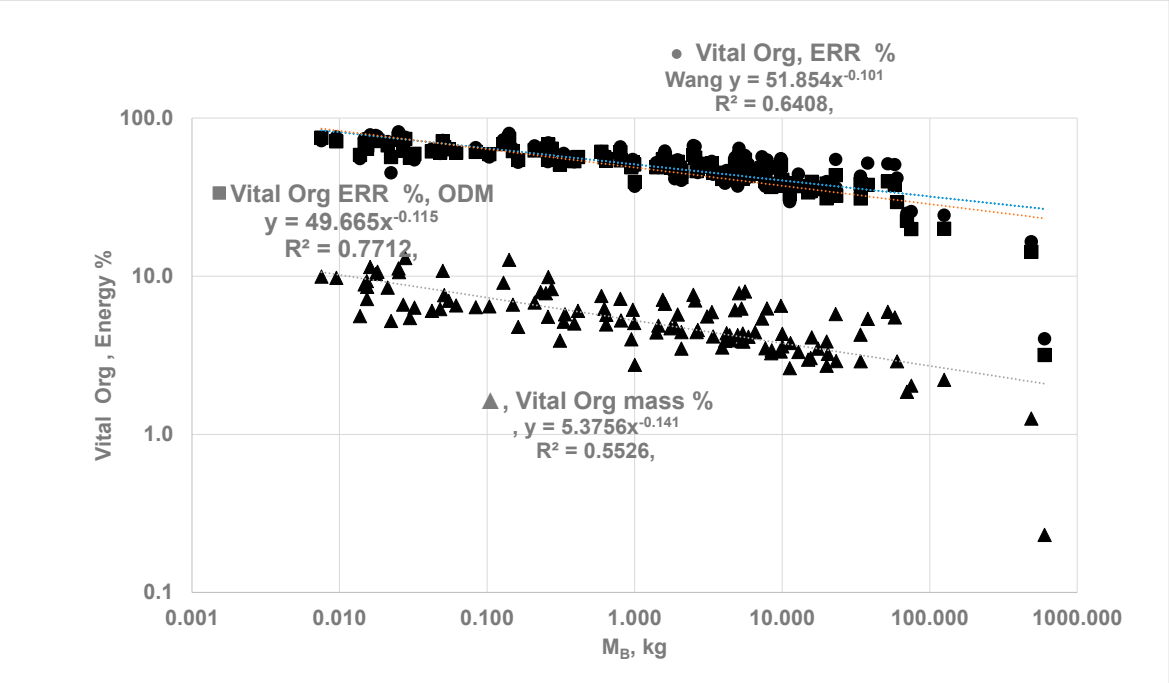

Figure 8. Comparison of vital organ mass percentage and energy contribution percentage: ODM vs. EAR for all organs. Energy contribution percentage by vital organs: $\%\, vit = \gamma_{vit}\, M_B^{\nu_{vit}}$. From ODM method (■): γ_{vit} = 49.67, ν_{vil} = -0.115. From EAR for all vital organs (●) [21]: γ_{vit} = 51.85, ν_{vil} = -0.101. (▲) vital organ mass percentage = 45.376 $M_B^{-0.141}$.

3.4. The Upper Metabolic Rate of Organ {UMR_B}, Maximum Metabolic Rate of Organ (MMR_k) and MMR_B of Whole-Body

Equation 2016 states that whole-body metabolic rate {$\dot{q}_B$} increases with the increase of $\eta_{eff,k}$, $\dot{q}_{k,m,iso}$ for metabolically dominant vital organs and the remaining tissue masses. The $\eta_{eff,k}$ is a function of O2 gradients within cell clouds; steeper the gradients lower is $\eta_{eff,k}$. Furthermore, $\dot{q}_B$ of aby BS is a strong function of $SOrMR_k$ {= $\eta_{eff,k}$ $\dot{q}_{k,m,iso}$ }, and $\dot{q}_{k,m,iso}$ is affected by $Y_{O2,CC,s}$ which depends on the percentage of capillaries perfused at the CC surface. .

A). Hypothetical Upper Metabolic Rates of Organs and whole body

The resting or basal metabolic rate (BMR) is based on oxygen consumption, typically with partial perfusion from capillaries. What if there is no oxygen concentration gradient? what is the effect of O2 gradients on " b"? Would this result in an isometric scaling law (b = 1 or b′ = 0), despite differences in organ masses? Mathematically, it can be shown that b ≠ 1 or b′ ≠ 0 due to differing $SOrMR_k$ of organs, rather than differences in organ masses. By setting $\eta_{eff,k}$ = 1 for all organs, a hypothetical upper metabolic rate (UMR) for the whole body can be obtained. By setting $\eta_{eff,k}$ = 1 for all vital organs, two cases were studied; using EAR for RM, the whole-body allometric relation is given as $\dot{q}_{B,UMR} = a_{UMR}\, M_B^{\,b_{UMR}} = 6.282\, M_B^{\,0.864}$ where a_{UMR} = 6.28, b_{UMR} = 0.864 {Figure 9}; it is apparent that "b" increases from 0.747 to 0.864 in absence of O_2 gradients. As such , the difference between $\dot{q}_{B,UMR}$ and $\dot{q}_B$ is due to the effects of O_2 gradients within vital organs.

 doi:10.20944/preprints202503.0386.v1

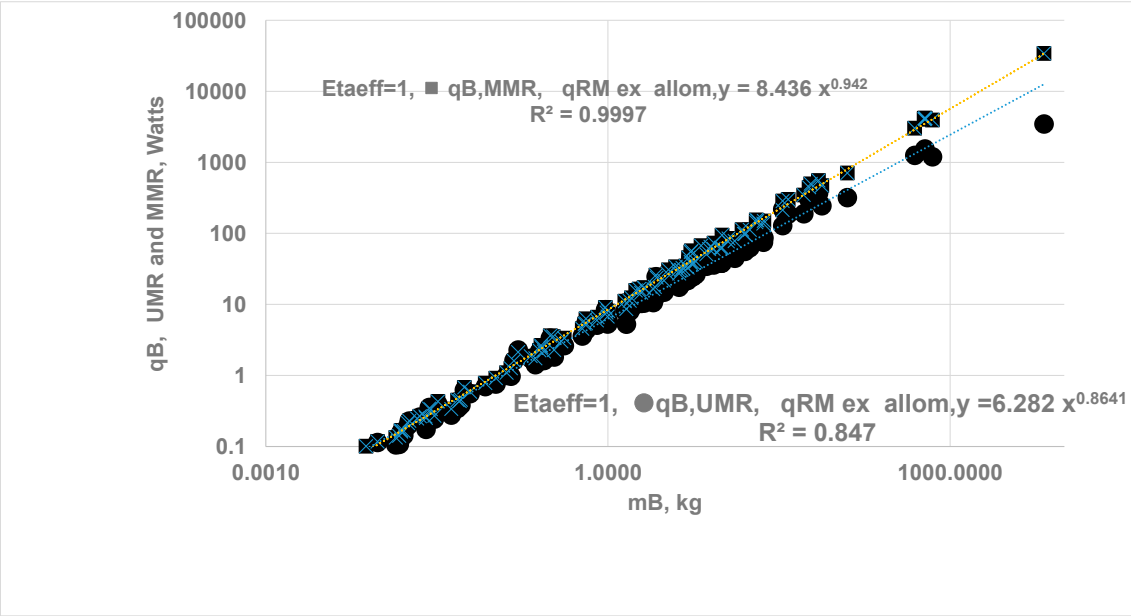

Figure 9. Comparison of UMR of of BS ($\dot{q}_{B,UMR}$, η_{eff} = 1) with MMR of BS { $\dot{q}_{B,MMR}$, η_{eff} = 1, Perf. Ratio}. The ODM based BMR with finite $\eta_{eff,k}$ yields Kleiber's law: $\dot{q}_B = 2.963\, M_B^{0.747}$, all $\dot{q}_B$ in Watts , $\dot{q}_{B,UMR} = a_{UMR}\, M_B^{b_{UMR}}$, (■) $\mathbf{a}_{UMR}$ = 6.282, $\mathbf{b}_{UMR}$ = 0.864 with $\dot{q}_{B,UMR}$ at isolated rates and $\dot{q}_{RM,m}$ following allometric law. The MMR vs MB is higher compared to UMR primarily due more perfusion of blood to SM and affected by $Y_{O2,CC,s}$ at CC surface is affected by more capillary perfusion for SoMRk. With $\dot{q}_{B,MMR} = a_{MMR}\, M_B^{b_{MMR}}$,: a_{MMR} = 8.436, b_{MMR} =0.942.

B). Maximum Metabolic Rates of Organs:

For maximal O_2 consumption (VO_2max), increased blood flow rates lead to higher capillary perfusion percentage, thereby increasing $Y_{O2,CC,s.}$ Since $\dot{q}_B = |\dot{Q}_B| + \dot{W}_B$ increases during exercise, both $\dot{W}_B$ { ATP work} and | $\dot{Q}_B$ | { heat loss from skin } must also increase, leading to a rise in internal temperature due to an increased | $\dot{Q}_B$ | nd ATP, or "work." This rise | $\dot{Q}_B$ | is accompanied by increased blood flow through the outer skin to enhance heat dissipation. The primary organs contributing to MMR are the heart and SM.

The cardiac output is approximately 5–6 LPM, with capillaries partially perfused on CC surface { about 25-30% of capillaries in vital organs and 15-25% in SM} . At rest, about 80% of the blood pumped by the heart flows through the four vital organs [54]. The *b* for BMR ranges from 0.66-0.75. Ref. [45] reports the percentage of capillaries perfused for organs falls within the 25-25% range.

Under exercise, cardiac output increases to approximately 25-35 LPM. During exercise, kidney perfusion accounts for 20-25% of resting blood flow [53,54] i.e. the flow though kidneys decrease under exercise {see Table 2} . The increased ERR ($\dot{q}_{B,MMR}$) is driven by a higher percentage of perfused capillaries (almost 100% exercise [55]) and decreased vascular resistance due to an increased diameter of small arteries (100–300 µm) [56], which increases blood supply rates, thus affecting the scaling law for $\dot{q}_{B,MMR}$. Further blood flow is diverted from various organs (e.g., stomach, kidneys). SM, which comprises about 40 % of the body mass, is almost 100% perfused during exercise. The increased O_2 delivery during exercise is also due to a lower pH (due to increased CO_2, or increased acidity), reduced oxy-Hb affinity, and hence, an increased release of O_2 from Hb which promotes higher $Y_{O2,CC,s}$. The OEF increases from 0.25-0.33 [54,61] at rest to almost 0.75 [54] for MMR.

 doi:10.20944/preprints202503.0386.v1

Since SM plays a major role in metabolism during exercise, allometric laws for mass of SM vs. M_B and increased blood flow are used in the ODM model: i) Prange's SM mass in kg: $m_{SM} = 0.061\ M_B^{1.09}$ [62] (M_B from 0.01 to 10,000 kg); ii) Kayser: $m_{SM} = 0.093\ M_B^{1.142}$ [63]; iii) Painter: $m_{SM} = 0.0961\ M_B^{1.06}$ [15]; iv) White: $m_{SM} = 0.0645\ M_B^{1.02}$ [64]; hence, 5.1 kg for a 58 kg person according to the Prange law but 9.6 kg according to the Kayser law, but the literature suggest SM is 24.4 kg for a 58 kg person [65].

For the ODM model during exercise, $m_{RM,ex} = M_B - m_{vit} - m_{SM}$. According to the ODM hypothesis, the increase in MMR is due to an increased O_2 supply to organs {particularly to SM and Heart} , with a higher perfusion percentage on the CC surface, thus increasing $Y_{O2,CC,s}$ and possibly due to an increased $\eta_{eff,CC}$ (See Section 4.8 in Ref. [66]} originating from an increased pO_2. With the following relations,

$$\left(\frac{Y_{O2,cc,s,Ex}}{Y_{O2,cc,s,Rest}}\right)_k = \left\{\frac{Blood\ \ Flow to\ organ\ k\ \ Exercise}{Blood\ \ Flow to\ k\ under\ \ Rest}\right\},\ k = Kids,\ H, Br, L,\ SM$$

$$\dot{q}_{k,m,Ex} = \left\{\dot{q}_{k,m,Rest}\left(\frac{Y_{O2,cc,s,Ex}}{Y_{O2,cc,s,Rest}}\right)_k\right\},\ \dot{q}_{SM,Ex} = \left\{\dot{q}_{SM,Rest}\ \frac{Y_{O2,cc,s,Ex}}{Y_{O2,cc,s,Rest}}\right\},\left\{\dot{q}_{RM,Ex,m}\right\} = \left\{\dot{q}_{RM,m}\right\}$$

$$\dot{q}_{SM,m,Rest} = \dot{q}_{RM,m,} = a_{RM}\ M_B^{\ b_{RM}} = e_{RM,6}\ M_B^{\ f_{RM,6}}\quad a_{RM} = e_{k,6} = 1.45,\ b_{RM} = f_{k,6} = -0.17,$$

For predicting MMR using the ODM model, perfusion ratios are used {Table 2} . The myoglobin(Mb) which aids in transport of O2 in H and SM increases during exercise indicating an increase of diffusivity "D"{i.e lower $G_{OD,k}$, k=H, SM} and the core cells may also get O2 decreasing OD and increasing $\{\eta_{eff,CC}\}_k$. Highest possible value $\{\eta_{eff,CC}\}_k$ is 1 for SM and H. Thus. the following parametric studies have been conducted:

a) The $\{\eta_{eff,CC}\}_k$ is finite for vital organs but isolated metabolic rate is altered due to change in capillary perfusion ratio (Equation 2420, Table 2 }: reduced for kidneys (0.55) and liver (0.67) but increased for H (3) , SM (10.4) and RM-ex (1.16). For SM and RM-ex, the SOrMRk are given by the product of allometric laws of RM as at rest and perfusion ratio. Figure 9 compares the results for $\dot{q}_{B,MMR}$ under ODM with the literature data for $\dot{q}_{B,MMR}$. If $\dot{q}_{B,MMR} = a_{MMR}\ M_B^{\ b_{MMR}}$, a $_{MMR}$= 4.015 and b_{MMR} = 0.798. The slope under exercise is steeper than the slope under rest.

b) The $\eta_{eff,CC}$ is set to 1 for all vital organs and SM {i.e no O2 gradient during exercise} but RM-ex given by allometric law with correction for perfusion ratio of 1.16. Even if O2 gradients are present for organs other than H and SM, results may not change since metabolic rate from SM dominates. a $_{MMR}$= 8.436 and b_{MMR} = 0.942, $\eta_{eff,k}$=1.

Preprints.org (www.preprints.org) | NOT PEER-REVIEWED | Posted: 5 March 2025 doi:10.20944/preprints202503.0386.v1

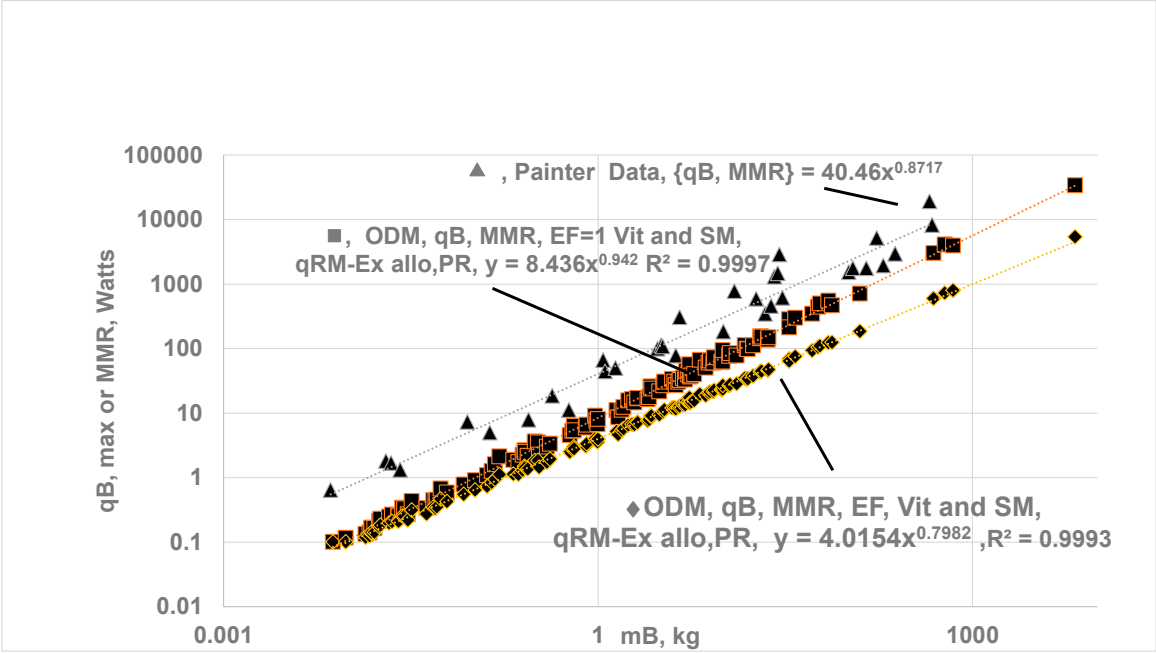

Figure 10. Comparison of MMR ($\dot{q}_{B,MMR}$, ♦ and ●), with the literature data (▲) on MMR of BS vs. body mass, M_B. M_B from 0.01 to 10,000 kg. $\dot{q}_{B,MMR} = a_{MMR} M_B^{b_{MMR}}$. The ODM based BMR with finite $\eta_{eff,k}$ yields Kleiber's law: $\dot{q}_B = 2.963\, M_B^{0.747}$, all in Watts , MMR : a) allometry predicted ,SM mass in kg: $m_{SM} = 0.061\, M_B^{1.09}$ [62] . $m_{RM\text{-}Ex} = M_B - m_{vit} - m_{SM}$ $\dot{q}_{RM-ex} = a_{RM-ex} M_B^{b_{RM-ex}}$. a) ♦ Vit organ with finite ηeff, $\dot{q}_{SM,m}$ and $\dot{q}_{RM-Ex,m}$ follow EAR, Perf. Ratio of Table 2 used, $a_{SM} = a_{RM}$ $b_{SM} = b_{RM}$ $a_{MMR} = 4.015$ $b_{MMR} = 0.798$, b) ● Assumed ηeff,k =1 for all vital organs and SM; RM-ex allom. Law of RM , $a_{RM\text{-}ex} = a_{RM}$, $b_{RM\text{-}ex} = b_{RM}$ {Table 1}.., $a_{MMR} = 8.436$ $b_{MMR} = 0.942$, Painter data from Literature in $V_{O2,max}$: $\dot{q}_{B,MMR}$ in watts $= 0.342\, V_{O2max}$ (mL/min) assuming 1 mL of O2 releases 20.5 J, For Painter data , $a_{MMR} = 40.46$ $b_{MMR} = 0.872$.

Validation of ODM Based MMR Allometry:

i) The predicted values for b_{MMR} range from 0.798 to 0.942 with an average of 0.87. The upper value of b_{MMR} indicates almost isometric law. It is believed that MMR must follow an isometric law since the "cost" of transportation (e.g., tread mill, jogging) must be proportional to body mass, meaning SMMR {specific maximum metabolic rate, W/kg} must not differ between smaller and larger species during exercise. Ref. [8] states that when a 20 g mouse and 500 kg racehorse run at their maximum capacity, their specific maximal metabolic rate (W/g) is nearly the same. This finding agrees with the ODM model, indicating all cells within an organ are subjected to oxygen concentrations close to their highest possible values.

ii) The literature data mostly reports $\dot{V}_{O2max}$ {mL of O2 per min} vs M_B under exercise. It is converted into watts using HHV_{O2} of 20.5 J/mL of O2. $\dot{q}_{B,MMR} = 0.342\dot{V}_{O2max}$ where $\dot{q}_{B,MMR}$ in Watts and $\dot{V}_{O2max}$ in mL/min . Painter collected data on MMR for 32 mammalian BS ranging from 0.007 kg (pygmy mice) to 575 kg (cattle), found that $b_{MMR} = 0.872$ (95% CI : b_{MMR} = 0.812-0.931) found and attributes the increase from 0.75 at rest to 0.872 under exercise to the increased O_2 transport to cells with the heart as the limiting step [15]. Based on VO_2max [67] in

 doi:10.20944/preprints202503.0386.v1

mL/min, a_{MMR} = 40.46 b_{MMR} = 0.872 .Weibel et al. [16] conducted treadmill experiments in animals to measure VO_2 max (highest rate for 5 min) and reported a_{MMR} = 118 mL/min or 40.4 W, with b_{MMR} = 0.872 for 34 mammalian species, including both athletic and non-athletic groups (0.007 to 500 kg). They further reported b_{MMR} =0.942 for the athletic group {predicted upper value for bMMR when ηeff=1 for vital organs and SM} and 0.849 for non-athletic group [16]. Data from Talyor et al. [67] and Ref. [8] report b_{mMR} = 0.87 - 0.88 for homeotherm.

iii) Ref. [6], b_{MMR} = 0.872 or 7/8 (see Fig. 6 in Ref. [6]), [15] ; Agutter b_{MMR} = 0.86 [72]. Ref [68]: b_{MMR} = 0. for M_B =0.3 to 300 kg, but increases to 0.86 for M_B = 0.3 to 500 kg. Single Flow Network model b_{MMR} = 6/7 [58] . However the predicted aMMR is low compared to literature data. MMR is largely driven by the high MR of SM, and the predicted low values of a_{MMR} orignate from the allometric relation of SM and body mass used in the current ODM model. This model assumes a similar SM mass percentage relative to body mass across species, yielding low SM values for humans. According to Weibel and Hoppeler [16], SM is about 42% of body mass in the athletic wood mouse (small animal), 45% in the pronghorn and 25% in the goat, with an average of 36% of body mass. Further, skeleton mass varies significantly, with the shrew at 5% and the elephant at 25% [71]. These findings indicate a wide variation in SM mass across body sizes.

iv) The current results for MMR are validated further with the data reported by Midorikawa et al [65]. The VO_2max (during maximal exercise) of sumo wrestlers is about 30 mL/min/kg or 10.25 W/kg, attributed to SM, liver and kidneys [65]. For a 58 kg individual, reported data show $\dot{q}_{B,MMR}$ =1320 W, while the predicted value is $\dot{q}_{B,MMR}$ 446 W . Why do measured values exceed predictions from the ODM model ? The allometry for SM predicts a mass of 5.1 kg for 58 kg human, whereas the measured value is 24 kg for a 58 kg person! When the author used the actual SM mass of 24 kg (without using allometric SM mass) and $m_{RM\text{-}EX} = M_B - m_{SM} - m_{vit}$ = 58 - 24 - 5.4 = 28.6 kg, the predicted $\dot{q}_{B,MMR}$ increased to 1045 W ($\dot{q}_{RM,ex}$ =296 W, EAR) with reported data at $\dot{q}_{B,MMR}$ =1320 W.

3.4. A Method of Tracking $G_{ODk\ Number}$ for Organs During Growth of Humans or any other BS by Medical Personnel

If O_2 diffusion follows an increasingly tortuous path for certain populations as humans grow, the effective diffusion coefficient decreases, causing $G_{OD,k}$ variation to become much steeper than normal. This indicates higher ODM and a greater likelihood of energy release adaptation by the body via glycolysis at a specific $(G_{OD,k})_{gly}$. Thus, estimating $(G_{OD,k})$ as $M_B(t)$ during the growth is of interest. How can medical personnel determine $G_{OD,k}$?

I) Direct Method: Measure Organ Masses and known $SOrMR_k$ of RS-1: Measure blood flow rate and the change in O_2 concentration between the arterial and venous ends of the organ to estimate $OrMR_k$. Directly measure organ masses using CT scan or MRI, then estimate $SOrMR_k$ (=$OrMR_k$ / m_k) and compare with $SOrMR_k$ of the shrew (i.e., isolated). Estimate $\eta_{eff,k}$ and determine $G_{OD,\,k}$ of organ *k* using Equation 1613.

II) Ratio method for Same BS: Assume that ($G_{OD\,k}$ at any age / $G_{OD\,k}$ at birth) = (m_k / $m_{k,birth}$) $^{\ell\,k}$ if $G_{OD,k}$ at birth and $m_{k,birth}$ are known.Typically ℓ_k =2/3.

III) $G_{OD,k}$ for normal growth in terms of Body Mass data $M_B(t)$: The ODM method presents SOrMRk in terms of a powerful dimensionless parameter $G_{OD\,k}$, which is proportional to m_k^{ℓ}.

 doi:10.20944/preprints202503.0386.v1

Using the allometric law for organ masses (Equation 5), $G_{OD\,k} \propto M_B(t)^{\ell_k d_k}$, *t in years*

where ℓ_k =2/3 and d_k values are tabulated in Table 1.

IV) Ratio Method, $G_{OD,k}$ in terms of measured Organ Masses and Reference Species RS-2:
Assuming Rat Wistar as RS-2 and knowing $G_{OD,k}$ of RS-2, one can determine $G_{OD,k}$ if organ mass data is available.

$$\frac{G_{OD,k}(t)}{G_{OD,k,RS-2}} = \left\{ \frac{m_k(t)}{m_{k,RS-2}} \right\}^{\ell_k}, \quad \ell_k = \frac{2}{3}, \quad t \text{ in years} \tag{28}$$

For example, selecting organ masses for a 10 kg (or 1 year old) infant from Ref. [73], the estimated $G_{OD,k}$ values and corresponding $\eta_{eff,k}$ (in parentheses) are : 65 (0.33) for the kidneys, 148 (0.23) for the heart, 1,007 (0.092) for the brain, and 522 (0.13) for the liver. For a dog of similar 10 kg body mass, the brain is much smaller, resulting in a significantly lower $G_{OD,Br}$ (179) and a higher $\eta_{eff,Br}$ (0.21), leading to a higher metabolic rate per unit mass of the dog's brain compared to a human's. As a human grows to 70 kg, the $G_{OD,k}$ increases while $\eta_{eff,k}$ decreases. Using the same reference, the values become: 160 (0.22) for the kidneys, 520 (0.13) for the heart, 1,260 (0.082) for the brain, and 1,422 (0.077) for the liver. Note the rapid growth of the liver and slow growth of the brain for a healthy human. If organ mass $m_k(t)$ is measured as a function of age in years, then Equation 2824 can be used to estimate $G_{OD,k}$.

Organ $G_{OD,k}$# and Cancer: Since ODM promotes hypoxic conditions, with increased HIF activity and, consequently, decreased mitochondrial mass and oxygen consumption, the author speculates that ODM promotes a shift toward the glycolysis pathway for energy release, which may contribute to the onset of cancer. While literature data indicates a positive correlation between organ mass and the number of cancer cases [42], which is attributed to the link between excess fat in organs and obesity, the author speculates that an increasing $G_{OD,k}$# is an indication of increased oxygen deficiency, an increased HIF1α factor and a possible shift to the glycolysis pathway, similar to how elevated Prostate-Specific Antigen (PSA) levels are used as an indicator of prostate cancer (see Section on Future Work).

4. Summary and Conclusions

The earlier literature: i) adopted empirical allometric laws of organs and a heterogenous approach and EAR for allometry of all organs for estimating BMR of the whole body, yielding Kleiber's aM_B^b with *a = 3.216, b = 0.756, [21];* ii) raised several puzzles in biology, such as a) why F_k values are negative [3] in OMA for *k* = Kids, H, Br and L; and b) how organs "know" they are in a smaller or large body mass and adjust their metabolic rates accordingly. The author's previous work answered these puzzles by linking the field of ODC literature in engineering to ODM in biology [3]. The current ODM method applies the effectiveness factor relation from engineering literature in terms of G (or Ψ_T^2,Thiele Modulus^2), and modifies G as G_{OD} (G-oxygen-deficiency) for biological applications. It demonstrates that $G_{OD,k} \propto R_{CC,k}^2$ ($\propto m_{CC,k}^{2/3} \propto m_k^{2/3}$). The ODM hypothesis is extended for: i) predicting the specific $SOrMR_k$ of organ k for 114 BS using only the SOrMRk of two reference species (Shrew of 0.0076 kg: RS-1, Rat of 0.380 kg: RS-2) and organ and body masses of 116 species, ii) demonstration of Kleiber's power law ($\dot{q}_B = a\, M_B^{\ b}$) with a = 2.962, b = 0.747 for M_B = 0.0075 kg to 6,650, iii) illustration of the link between morphological traits and physiological traits in metabolic rates, iv) extension of the method to deduce the allometric law for maximal metabolic rate (MMR under exercise) and validation with literature data. Even if all cells are irrigated with the same O_2 concentration, the exponent *b* is not equal to 1 due to varying organ masses, but b = 1 if all organ masses are equal. Thus, ODM hypothesis aligns with Silva's [17] review, which suggests that the power law exponent *b* should vary between 2/3 and 1 based on 'metabolic level' (i.e., the organism's activity level or metabolic intensity). Allometric laws on maximum metabolic rate (MMR) vs. body

 doi:10.20944/preprints202503.0386.v1

mass M_B are also validated using the ODM approach, yielding an exponent of 0.87-0.92, as reported in biology literature. That is, MMR per kg body mass $\propto M_B$ (-0.13) to M_B (-0.08) {i.e. weak function of body mass }, appearing consistent (e.g., VO_2max/M_B in Ref. [8]), even though the SBMR (W/g body mass) of a 20 g mice is five times that of a 500 kg horse. A method for estimating the dimensionless $(G_{OD})_k$ for organs is "suggested" for use by medical personnel whether the increasing $(G_{OD})_k$ of organs indicate a progression toward oxygen deficiency. Note that glycolysis generates only 2 ATP per CH molecule and as such generation of 32 ATP (as in case of oxidation) requires 16 times more consumption of O2 and hence fall in CH level is an indication of likelihood of occurrence of cancer.

5. Future Work

1. Whether the secrets of Kleiber's law and maximal metabolic rate allometries in biology can be revealed from oxygen-deficient combustion engineering remains an open question. Additional supporting data are needed either to confirm or question the ODM hypothesis.
2. While the present study focuses on interspecific relations across 116 species, the approach may also apply to intraspecific relations, such as human growth from 2 kg to 70 kg. As organs grow, $G_{OD,\,k}$ can be monitored throughout the development process. Notably, human brain growth appears to deviate from the allometric laws for organ masses based on Wang's six-species data.
3. Collect statistical data to determine whether cancer development correlates with abnormal increases in $G_{OD,k}$ and assess its relationship with cancer occurrence.
4. Conduct future studies on the impact of RS-2 selection on Kleiber's law.
5. A more precise allometric relationship is needed for SM mass relative to body mass M_B since it directly affects the predicted MMR in the ODM model.
6. Develop a Krogh-type COA model incorporating the ODM method, define $G_{OD,k}$ for COA and evaluate whether Kleiber's law holds.
7. Gather data on cell reactivity, cell size, cell density and organ mass to estimate $G_{OD,k}$ using fundamental biological parameters.
8. While the current work follows a "downstream" hypothesis based on cell kinetics, the WBE employs an "upstream" flow network (or supply-side) hypothesis and optimization. Future work should aim to integrate these two hypotheses to understand their combined effects on mass fraction of O2 at the cell cloud surface $\{Y_{O2,cc,s}\}$.

Funding: This project was pursued purely out of curiosity after observing similarities between the specific energy release rate (SERR, W/kg of FC) from fuel (carbon) clouds with those from organs (cell clouds, W/kg of k) in biological systems. The research was conducted independently after the author's retirement from academia, with no funding sought from any federal agency. The author speculates that this work may be of interest to oncologists and could provide a meaningful contribution to society. However, the foundation for this research on group/oxygen-deficient combustion (ODC) of carbon clouds was laid by earlier funding from the U.S. Department of Energy, including DOE-Pittsburgh: DE-FG22-90 PC 90310, DE-FG 22-88 PC 88937, DE-FG 22-85 PC 80528 and Department of Energy –Morgantown: DOE- METC DE-AC21-86 MC 23256.

Contributions: As the sole contributor of this work, the author has approved it for publication.

Acknowledgements: Ms. Megan Simison of the J. Mike Walker '66 Department of Mechanical Engineering, Texas A&M University, for English editing of manuscript.

Conflict of Interest and other Ethics Statements: The author declares no conflict of interest.

 doi:10.20944/preprints202503.0386.v1

Acronyms

a	Normalization Constant in Kleiber's law $\dot{q}_B = a\ M_B^{\ b}$
b	allometric scaling exponent in Kleiber's law
BMA	Body mass based Allometry
BMR	Basal Metabolic Rate
CC	Cell Cloud
$C_{Ch,p}$	Characteristic O_2 consumption rate by particle in fuel cloud [3]
$C_{ch,\ cell}$	Characteristic O_2 consumption rate by a cell in cell cloud [3]
Cap	Capillary
Cap-IF	Interface between capillary and Interstitial Fluid (IF)
COA	Capillary on Axis
COS	Capillary On Surface
EAR	Empirical Allometric Relation
EQ	Encephalization Quotient
ERR	Energy release rate, W
FC	Fuel (particle) Cloud
IF	Interstitial Fluid (IF)
M_B	Body mass
MR	Metabolic Rate
MMR	Maximal Metabolic Rate
m	mass
n_{CC}	number density of cells, cells/m^3
n_{FC}	number density of fuel particle, particles/m^3
OD	Oxygen deficient/deficiency
ODC	Oxygen-Deficient Metabolism
ODM	Oxygen-Deficient Metabolism
OEF	Oxygen Extraction Fraction
OEM	Oxygen extraction Fraction
OMA	Organ Mass Based Allometry
OrM_k	Organ metabolic rate of organ k, = $SOrM_k$ x m_k , W
$q_{k,m}$	Metabolic rate of organ k per unit mass of organ, (W/kg of organ k)
q_M	Metabolic rate of whole body per unit mass of body, (W/kg of body)
RM	Remaining Mass , M_B- m_{vit}t
RM,Ex	Remaining Mass during exercise , M_B- m_{vit}t-m_{SM}
SATP	Standard Atm Temperature and Pressure, T = 25 C, P = 101 kPa
SBMR	Specific Basal Metabolic Rate (W/kg of body)
SERR	Specific Energy release rate (W/kg of cloud)
SM	Skeletal Muscle
$SOrMR_k$	Specific organ metabolic rate,
UMR	Upper Metabolic rate when O_2 gradient is zero
WBE	West, Brown and Enquist
Vit	vital organs
Y_{O2}	Oxygen mass fraction g of O_2 per g of mixture
$Y_{O2,CC,s}$	Oxygen mass fraction at surface of cell cloud
$Y_{O2,FC,s}$	Oxygen mass fraction at surface of fuel cloud

Appendix A

Table 3. Data on body and a mases (kg), Specific Organ Metabolic rates (W/k organ), and comparison of Whole-body metabolic rates from ODM and EAR. Empirical Allometric Rule (EAR), $\dot{q}_{k,m} = e_{k,6}\ M_B^{\ f_{k,6}},\ k = Kid, H, Br, L$.

	Species	M_B,kg	$\dot{q}_{kid,m}$ W/kg	$\dot{q}_{H,m}$ W/kg	$\dot{q}_{Br,m}$ W/kg	$\dot{q}_{L,m}$ W/kg	$\dot{q}_{RM,m}$ W/kg	$100xm_{kids}$kg	$100xm_H$, kg	$100xm_{Br}$, kg	$100xm_L$ kg	$100xm_{vit}$ kg	Vit ERR % ODM	Vit ERR % EAR,	$\dot{q}_B$ ODM W	$\dot{q}_B$ EAR, W
1	Shrew/Sorex araneus	0.00755	50.2	76.8	43.3	122.5	3.3	0.011	0.011	0.015	0.038	0.68	71.8	71.8	0.09	0.09
2	Crocidura russula	0.00953	49.2	74.7	41.9	115.1	3.2	0.013	0.008	0.017	0.055	0.86	75.7	75.7	0.09	0.11
3	Lasiurus borealis	0.01377	47.7	71.5	39.8	104.3	3.0	0.011	0.014	0.017	0.035	1.3	55.4	55.4	0.09	0.10
4	Lasionycteris noctivagans	0.01478	47.5	70.9	39.4	102.3	2.9	0.013	0.016	0.016	0.033	1.4	53.2	53.2	0.10	0.10
5	Mus musculus	0.01539	47.3	70.6	39.2	101.2	2.9	0.028	0.007	0.036	0.068	1.4	77.1	77.1	0.13	0.14
6	Myodes glareolus	0.01536	47.3	70.6	39.2	101.3	2.9	0.024	0.01	0.035	0.067	1.4	74.1	74.1	0.13	0.14
7	Microtus agrestis	0.01531	47.3	70.6	39.2	101.4	2.9	0.017	0.012	0.039	0.063	1.4	69.8	69.8	0.12	0.14
8	Neomys fodiens	0.01616	47.1	70.2	38.9	99.9	2.9	0.022	0.014	0.025	0.055	1.5	66.6	66.6	0.12	0.13
9	Blarina brevicauda	0.01764	46.8	69.5	38.4	97.6	2.8	0.021	0.018	0.032	0.093	1.6	71.8	71.8	0.15	0.17
10	Apodemus sylvaticus	0.01807	46.7	69.3	38.3	97.0	2.8	0.026	0.014	0.057	0.11	1.6	78.1	78.1	0.17	0.20
11	Microtus	0.02119	46.1	68.0	37.4	92.9	2.8	0.036	0.015	0.058	0.11	1.9	77.3	77.3	0.18	0.20
12	Peromyscus leucopus	0.02239	45.9	67.5	37.1	91.6	2.7	0.03	0.015	0.074	0.12	2	76.4	76.4	0.19	0.22
13	Apodemus flavicollis	0.02513	45.4	66.6	36.5	88.8	2.7	0.034	0.018	0.061	0.1	2.3	70.9	70.9	0.19	0.20
14	Nyctalus noctula	0.02532	45.4	66.6	36.5	88.6	2.7	0.013	0.037	0.032	0.05	2.4	45.0	45.0	0.15	0.15
15	Microtus arvalis	0.02703	45.1	66.0	36.1	87.1	2.6	0.055	0.019	0.039	0.19	2.4	81.7	81.7	0.25	0.28
16	Mouse	0.02797	45.0	65.8	36.0	86.3	2.6	0.051	0.016	0.05	0.18	2.5	80.4	80.4	0.24	0.27
17	Gerbillus perpallidus	0.02998	44.8	65.2	35.6	84.7	2.6	0.027	0.013	0.058	0.1	2.8	65.1	65.1	0.19	0.20
18	Mustela nivalis	0.03219	44.5	64.7	35.3	83.1	2.6	0.043	0.036	0.18	0.16	2.8	75.5	75.5	0.27	0.31
19	Acomys minous	0.0423	43.5	62.6	33.9	77.2	2.5	0.032	0.018	0.09	0.09	4	57.2	57.2	0.22	0.22
20	Jaculus jaculus	0.04804	43.0	61.7	33.3	74.6	2.4	0.029	0.045	0.12	0.11	4.5	54.3	54.3	0.27	0.27
21	Rhabdomys pumilio	0.05002	42.9	61.4	33.1	73.8	2.4	0.041	0.021	0.06	0.18	4.7	63.6	63.6	0.29	0.30

doi:10.20944/preprints202503.0386.v1

22	Talpa europaea	0.05117	42.8	61.2	33.0	73.4	2.4	0.036	0.031	0.1	0.15	4.8	59.6	59.6	0.29	0.29
23	Glaucomys volans	0.05495	42.5	60.7	32.7	72.0	2.4	0.059	0.056	0.19	0.29	4.9	72.1	72.1	0.40	0.45
24	Arvicola terrestris	0.06168	42.1	59.9	32.1	69.8	2.3	0.07	0.028	0.11	0.26	5.7	69.9	69.9	0.38	0.39
25	Glis glis	0.08386	41.1	57.8	30.8	64.3	2.2	0.068	0.048	0.15	0.32	7.8	64.3	64.3	0.47	0.48
26	Tamias striatus	0.10377	40.4	56.3	29.8	60.7	2.1	0.081	0.066	0.24	0.29	9.7	59.9	59.9	0.52	0.52
27	Octodon degus	0.12921	39.6	54.9	28.9	57.3	2.0	0.11	0.041	0.19	0.48	12.1	64.9	64.9	0.64	0.64
28	Tupaia glis	0.14107	39.3	54.3	28.6	55.9	2.0	0.11	0.117	0.34	0.34	13.2	56.7	56.7	0.65	0.66
29	Rat	0.1496	39.1	54.0	28.3	55.1	2.0	0.14	0.07	0.23	0.92	13.6	72.9	72.9	0.86	0.94
30	Cebuella Cebuella	0.16266	38.9	53.4	28.0	53.8	2.0	0.19	0.086	0.44	1.35	14.2	79.9	79.9	1.06	1.25
31	Rattus norvegicus	0.20987	38.1	51.8	27.0	50.3	1.9	0.15	0.087	0.23	0.92	19.6	64.2	64.2	0.97	1.00
32	Cheirogaleus medius	0.23103	37.8	51.3	26.6	49.0	1.9	0.1	0.093	0.28	0.63	22	52.4	52.4	0.89	0.88
33	Rat	0.25004	37.5	50.8	26.3	48.0	1.8	0.21	0.094	0.2	1.2	23.3	66.6	66.6	1.13	1.18
34	Mustela erminea	0.2585	37.4	50.6	26.2	47.6	1.8	0.23	0.25	0.57	1	23.8	62.8	62.8	1.19	1.27
35	Helogale parvula	0.2603	37.4	50.5	26.2	47.5	1.8	0.25	0.15	0.52	1.11	24	67.0	67.0	1.20	1.27
36	Sciurus vulgaris	0.2742	37.2	50.2	26.0	46.8	1.8	0.17	0.17	0.63	0.55	25.9	52.9	52.9	1.02	1.04
37	Callithrix jacchus	0.3118	36.8	49.5	25.5	45.2	1.8	0.29	0.28	0.73	1.78	28.1	69.6	69.6	1.55	1.73
38	Saguinus fuscicollis	0.3304	36.6	49.1	25.3	44.5	1.7	0.19	0.33	0.78	1.44	30.3	61.2	61.2	1.47	1.60
39	Rat	0.3372	36.6	49.0	25.2	44.3	1.7	0.23	0.1	0.19	0.8	32.4	51.9	51.9	1.14	1.10
40	Rat (Wistar)	0.3901	36.1	48.2	24.7	42.6	1.7	0.28	0.11	0.19	1.43	37	59.7	59.7	1.43	1.44
41	Sciurus niger	0.4127	36.0	47.9	24.5	42.0	1.7	0.3	0.25	0.75	1.07	38.9	56.0	56.0	1.48	1.51
42	Sciurus carolinensis	0.5959	34.9	45.8	23.3	38.0	1.6	0.32	0.28	0.75	1.64	56.6	52.8	52.8	1.92	1.93
43	Saguinus oedipus	0.6237	34.8	45.6	23.1	37.6	1.6	0.31	0.37	1	2.09	58.6	55.7	55.7	2.12	2.21
44	Mustela putorius	0.64	34.7	45.4	23.0	37.3	1.6	0.4	0.48	1.04	2.88	59.2	61.3	61.3	2.39	2.60
45	Leontopithecus chrysomelas	0.642	34.7	45.4	23.0	37.3	1.6	0.41	0.38	1.32	1.89	60.2	57.1	57.1	2.15	2.26
46	Guinea pig	0.7996	34.0	44.3	22.3	35.2	1.5	0.56	0.23	0.47	2.7	76	57.6	57.6	2.46	2.49
47	Potorous tridactylu	0.8091	34.0	44.2	22.3	35.0	1.5	0.62	0.48	1.14	2.37	76.3	56.7	56.7	2.55	2.65
48	Erinaceus europaeus	0.9493	33.6	43.4	21.8	33.6	1.5	0.89	0.55	0.43	4.96	88.1	65.7	65.7	3.27	3.59
49	Sylvilagus floridanus	0.972	33.5	43.3	21.7	33.4	1.5	0.63	0.48	0.79	3.2	92.1	55.4	55.4	2.91	3.00
50	Ondatra zibethicus	0.9915	33.4	43.2	21.6	33.2	1.5	0.58	0.3	0.47	2.6	95.2	50.6	50.6	2.70	2.67
51	Saimiri boliviensis	1.0026	33.4	43.1	21.6	33.1	1.5	0.67	0.65	2.9	1.94	94.1	54.7	54.7	2.87	3.14

doi:10.20944/preprints202503.0386.v1

52	Martes foina	1.406	32.5	41.4	20.6	30.2	1.4	0.73	0.98	1.9	3.49	133.5	49.0	49.0	3.72	3.92
53	Mephitis mephitis	1.4488	32.4	41.3	20.5	30.0	1.4	0.66	0.6	0.98	1.74	140.9	37.0	37.0	3.17	3.11
54	Trichosurus vulpecula	1.5504	32.2	40.9	20.3	29.4	1.3	1.35	0.9	1.27	3.32	148.2	52.1	52.1	3.91	4.04
55	Martes martes	1.603	32.1	40.8	20.2	29.2	1.3	0.88	1.08	2.05	3.79	152.5	48.6	48.6	4.08	4.29
56	Cebus apella	1.7499	31.9	40.4	20.0	28.5	1.3	1.04	1.34	5.08	4.93	162.6	56.7	56.7	4.75	5.44
57	Eulemur macaco macaco	1.8753	31.7	40.0	19.8	28.0	1.3	1.42	0.91	2.42	7.78	175	61.8	61.8	5.22	5.76
58	Chrotagale owstoni	1.9598	31.6	39.8	19.6	27.7	1.3	1.28	1.16	2.33	4.41	186.8	50.1	50.1	4.72	4.97
59	Vulpes corsac	2.0752	31.4	39.6	19.5	27.2	1.3	0.88	2.17	3.41	3.56	197.5	41.2	41.2	4.82	5.31
60	Lemur catta	2.0746	31.4	39.6	19.5	27.2	1.3	1.12	1.17	2.28	7.29	195.6	54.4	54.4	5.33	5.76
61	Eulemur fulvus fulvus	2.5002	31.0	38.7	19.0	25.9	1.2	0.95	1.18	2.25	4.34	241.3	40.3	40.3	5.21	5.31
62	Felis silvestris	2.573	30.9	38.6	18.9	25.7	1.2	1.54	1.03	3.81	5.02	245.9	49.9	49.9	5.62	5.93
63	Didelphis virginiana	2.6336	30.8	38.5	18.8	25.6	1.2	2.29	1.21	0.83	15.73	243.3	66.9	66.9	7.24	8.35
64	Aonyx cinerea	2.675	30.8	38.4	18.8	25.4	1.2	3.06	1.51	3.59	10.64	248.7	66.1	66.1	6.97	7.97
65	Leopardus geoffroyi	3.1002	30.4	37.7	18.4	24.5	1.2	3.07	1.6	3.21	5.84	296.3	54.6	54.6	6.61	7.12
66	Lepus europaeus	3.3386	30.2	37.4	18.2	24.0	1.2	1.85	2.89	1.48	9.04	318.6	45.2	45.2	7.26	7.86
67	Dasyprocta punctata	3.4002	30.2	37.3	18.2	23.9	1.2	2.13	3.63	2.28	10.88	321.1	48.8	48.8	7.81	8.81
68	Potos flavus	3.9203	29.8	36.7	17.8	23.0	1.2	1.44	2.11	3.11	16.57	368.8	53.1	53.1	8.84	9.82
69	Dasyprocta azarae	4.1004	29.7	36.5	17.7	22.7	1.1	2.27	3.04	2.38	9.35	393	44.1	44.1	8.22	8.83
70	Varecia rubra	4.2004	29.6	36.4	17.6	22.5	1.1	2.24	1.81	3.57	7.22	405.2	43.7	43.7	7.87	8.21
71	Alouatta sara	4.3996	29.5	36.2	17.5	22.3	1.1	0.99	2.4	5.65	8.12	422.8	38.7	38.7	8.20	8.75
72	Monkey	4.5	29.5	36.1	17.5	22.1	1.1	2.1	2.3	4.2	11	430.4	46.5	46.5	8.85	9.48
73	Martes pennanti	4.7907	29.3	35.8	17.3	21.8	1.1	2.11	2.74	4.12	11.3	458.8	44.5	44.5	9.22	9.90
74	Trachypithecus vetulus	4.9996	29.2	35.7	17.2	21.5	1.1	1.54	1.92	7.2	9	480.3	42.3	42.3	9.03	9.64
75	Lutrogale perspicillata	5.1002	29.2	35.6	17.1	21.4	1.1	4.85	4.85	6.22	15.2	478.9	56.1	56.1	10.83	12.76
76	Chlorocebus pygerythrus	5.3005	29.1	35.4	17.1	21.2	1.1	1.21	4.26	8.08	8.9	507.6	37.1	37.1	9.58	10.70
77	Lutra lutra	5.3253	29.1	35.4	17.0	21.2	1.1	6.11	5.14	4.78	25.5	491	64.2	64.2	12.38	15.20
78	Proteles cristata	5.3998	29.0	35.3	17.0	21.1	1.1	2.43	9.06	3.99	18.2	506.3	42.4	42.4	11.44	13.97
79	Agouti paca	5.4599	29.0	35.3	17.0	21.0	1.1	2.22	1.76	3.21	14	524.8	45.5	45.5	10.04	10.49

doi:10.20944/preprints202503.0386.v1

80	Macaca nigra	5.5997	28.9	35.2	16.9	20.9	1.1	1.86	2.39	10.52	9.5	535.7	44.1	44.1	9.95	10.98
81	Puma yagouaroundi	5.9007	28.8	35.0	16.8	20.6	1.1	3.91	2.96	4.3	11.6	567.3	47.1	47.1	10.60	11.40
82	Hylobates concolor	6.5502	28.6	34.5	16.5	20.0	1.1	3.52	5.82	13.78	29.3	602.6	57.9	57.9	14.08	17.55
83	Prionailurus viverrinus	7.3003	28.3	34.1	16.3	19.4	1.0	5.59	3.35	5.29	16	699.8	51.0	51.0	12.78	13.99
84	Macropus agilis	7.7003	28.2	33.9	16.2	19.2	1.0	4.63	6.02	3.08	20.3	736	45.7	45.7	13.71	15.33
85	Lontra canadensis	7.9003	28.1	33.8	16.1	19.0	1.0	7.47	5.41	4.25	25.5	747.4	56.8	56.8	14.83	17.15
86	Dolichotis patagonum	8.4296	28.0	33.5	16.0	18.7	1.0	3.6	6.51	3.65	15.8	813.4	37.0	37.0	13.72	15.00
87	Symphalangus syndactylus	8.5002	28.0	33.5	15.9	18.7	1.0	4.37	5.15	14.3	29.4	796.8	54.3	54.3	15.87	18.81
88	Colobus guereza	9.7498	27.6	32.9	15.6	18.0	1.0	2.33	3.7	8.65	17.1	943.2	36.5	36.5	14.79	15.66
89	Felis chaus	9.7999	27.6	32.9	15.6	18.0	1.0	8.19	4.83	4.97	15.3	946.7	48.0	48.0	15.26	16.77
90	Lynx canadensis	10.0003	27.6	32.8	15.6	17.9	1.0	5.49	3.88	8.26	15.8	966.6	43.4	43.4	15.26	16.45
91	Dog	10	27.6	32.8	15.6	17.9	1.0	7	8.5	7.5	42	935	55.4	55.4	18.73	22.64
92	Hystrix indica	11.2543	27.3	32.4	15.3	17.3	1.0	5.24	5.62	4.07	25.5	1085	42.0	42.0	17.39	18.81
93	Theropithecus gelada	11.4021	27.3	32.3	15.3	17.3	1.0	3.8	7.72	14.09	23.6	1091	40.9	40.9	17.83	20.31
94	Pudu puda	12.898	27.0	31.9	15.0	16.7	0.9	1.99	5.05	6.16	20.6	1256	29.5	29.5	17.75	18.41
95	Gazella gazella	14.9969	26.7	31.3	14.7	16.0	0.9	4.06	12	7.93	32.7	1443	34.9	34.9	21.79	24.58
96	Castor fiber	15.5662	26.6	31.2	14.6	15.9	0.9	7.83	4.4	4.89	34.5	1505	44.1	44.1	21.97	23.47
97	Macaca arctoides	15.87	26.5	31.1	14.6	15.8	0.9	5	6.1	11.8	24.1	1540	35.8	35.8	21.30	22.85
98	Lynx lynx	17.5008	26.3	30.7	14.4	15.4	0.9	7.95	9.3	9.43	26.4	1697	37.4	37.4	23.35	25.65
99	Capreolus capreolus	20	26.0	30.3	14.1	14.8	0.9	8	16	10	48	1918	39.3	39.3	27.93	32.35
100	Cuon alpinus	19.9964	26.0	30.3	14.1	14.9	0.9	7.64	15.8	11.6	34.6	1930	35.2	35.2	26.68	30.54
101	Dog	20.388	26.0	30.2	14.1	14.8	0.9	9.2	15.3	9.6	44.7	1960	39.6	39.6	27.98	32.17
102	Mandrillus sphinx	23.0249	25.7	29.8	13.8	14.3	0.9	4.99	7.6	16.8	33.1	2240	32.2	32.2	27.95	29.87
103	Papio hamadryas	23.2493	25.7	29.7	13.8	14.3	0.9	8.03	10.3	17.4	39.2	2250	37.4	37.4	29.35	32.45
104	Zalophus californianus	33.9579	24.9	28.4	13.1	12.9	0.8	20.59	16.8	31	127.4	3200	54.7	54.7	45.67	56.18
105	Hydrochaeris hydrochaeris	33.9875	24.9	28.4	13.1	12.9	0.8	10.35	10.4	8.4	69.6	3300	36.1	36.1	39.32	42.20
106	Canis lupus chanco	38.0209	24.7	28.1	12.9	12.5	0.8	20.69	30.3	14	97.1	3640	42.9	42.9	46.66	56.35
107	Sheep	52.006	24.0	27.0	12.3	11.5	0.8	16	28	10.6	96	5050	32.5	32.5	54.93	61.68

doi:10.20944/preprints202503.0386.v1

108	Reference women	58.015	23.8	26.7	12.1	11.2	0.7	27.5	24	120	140	5490	51.8	51.8	65.07	83.63
109	Human	59.97	23.8	26.6	12.1	11.1	0.7	25	32	130	170	5640	51.4	51.4	68.58	90.32
110	Reference man	70.04	23.5	26.1	11.8	10.6	0.7	31	33	140	180	6620	50.8	50.8	75.95	98.83
111	Panthera tigris altaica	74.9716	23.3	25.9	11.7	10.4	0.7	42.46	30.5	34.2	110	7280	41.6	41.6	72.84	84.70
112	Hog	125.33	22.3	24.4	10.9	9.1	0.6	26	35	12	160	12300	25.0	25.0	102.80	109.95
113	Dairy cow	487.9	20.0	20.8	9.0	6.3	0.5	116	188	40	646	47800	25.6	25.6	308.50	353.68
114	Horse	600.28	19.6	20.3	8.7	6.0	0.5	166	425	67	670	58700	24.2	24.2	366.40	457.67
115	Steer	699.8	19.4	19.9	8.5	5.7	0.5	100	230	50	500	69100	16.5	16.5	392.43	434.45
116	Elephant	6650.4	16.1	15.2	6.2	3.1	0.3	120	220	570	630	7E+05	4.0	4.0	2292.18	2327.20

doi:10.20944/preprints202503.0386.v1

 doi:10.20944/preprints202503.0386.v1

Appendix B

Step 1: First, select the Reference Species (RS-1) with the lowest body mass

RS-1: shrew, M_B= 7.6 g. Since there are very few cells in each organ, each cell is assumed to operate in isolation mode, with Y_{O2} for all cells within CC = $Y_{O2,s,CC}$; $\eta_{eff,k} \approx 1$ for RS-1. Hence, $SOrMR_k$ of RS-1 under isolated condition is the same as $\{SOrMR_k\}_{iso}$. They are estimated using 6 species corelations : $\dot{q}_{k,m} = e_{k,6}\ M_B^{\ f_{k,6}}, \{\dot{q}_{k,m}\}_{RS-1} = \{\dot{q}_{k,m}\}_{iso}\ of\ any\ BS$ = 50.2 W/kg , 76.8, 43.3 and 122.5 W/kg of k, k= Kid, H, Br and L ;. The 6 species six species correlations are used to estimate $SOrMR_{k,RS-1}$ [21]. See first row, Table 3.

Step 2: Select RS-2, whose body mass is much larger than that of Shrew. Thus RS-2 is selected as Rat Wistar, 390 g. Note that SOrMRk data for RS-2 is available. However EAR is used to estimate $\{\dot{q}_{k,m}\}_{RS-2} = \left\{e_{k,6}\ M_B^{\ f_{k,6}}\right\}_{RS-2}$ Body mass is much larger and hence contains organs of greater mass (note dk > 0 for organ size allometry, Equation 5). As a result, the cells in the vital organs of RS-2 operate under OD mode, exposed to varying Y_{O2} concentrations, with $G_{OD,k}$ being much higher compared to RS-1 {steeper part of $\eta_{eff,k}$ vs. $G_{OD,k}$, Zone II,Figure 2}. $\{\dot{q}_{k,m}\}_{RS-2}$ =36.1, 48.2, 24.7 and 42.6 W/kg for k=Kid, H, Br and L. $\dot{q}_{RM,m} = 1.7$ as given by EAR for RM.) and hence $\eta_{eff,k} < 1$. Zone 1 is avoided for RS-2, as small variation in η_{eff} near 1 cause large variations in $G_{OD,k}$.

$$\eta_{eff,k,RS-2} = \frac{\dot{q}_{k,m\ RS-2}}{\dot{q}_{k,m,RS-2,iso}} \approx \frac{SOMR_{k,RS-2}}{SOMR_{k,RS-1}} = \frac{\dot{q}_{k,m\ RS-2}}{\dot{q}_{k,m,RS-1}}\ k = Kids, H, Br, L \tag{29}$$

In absence of direct data on SOrMRk or $\{\dot{q}_{k,m,\ RS\text{-}2}\}$ of RS-2, the EAR-6 correlations are used to estimate $SOrMR_{k,RS-2}$. Estimate $\eta_{eff,k}$ for RS-2 as 0.72, 0.63, 0.57, 0.35 for k=Kid, H, Br and L.The corresponding masses of vital organs are 0.0028, 0.0011, 0.0019 and 0.0143 kg.

Step 3: Use Equation 1613 to estimate $(G_{OD,k})_{RS-2}$ (or $\left(\Psi_{T,k}\right)^2_{RS-2}$) : 6.93, 11.59, 15.45, 56.6 for k= Kid, H, Br and L.

Step 4: Since $G_{OD,k} \propto R_{CC,k}^2$ and hence $G_{OD,k} \propto m_{CC,k}^{(2/3)}$ than for any BS,

$$\frac{\left(G_{OD,k}\right)_{BS}}{\left(G_{OD,k}\right)_{RS-2}} = \left(\frac{m_{k,BS}}{m_{k,RS-2}}\right)^{(2/3)}\ since\ \left(R_{k,CC}\right)_{BS} \propto m_{k,BS},\ \ k = Kids, H, Br, L, BS \neq RS-1 \tag{30}$$

E.g. Select BS as dog of mass 10 kg., organ mass, mk= 0.07, 0.085, 0.075, 0.42; Using Equation 3026, estimate $(G_{OD,k})_{dog}$ =6.93*(0.07/0.0028) $^{(2/3)}$= 59.2 for kid; similarly 210.4, 179.1, 538.8 for H, Br and L and corresponding $\eta_{eff,k}$ are: 0.55, 0.43,0.36, 0.15.; $\{\dot{q}_{kid,m}\}_{dog}$ = 0.55*50.2= 27.6 W/kg of kid. Similarly $\{\dot{q}_{k,m}\}_{dog}$ = 32,.8, 15.6, 17.9 W/lg for H, Br and L.

Step 5: Summing up MR of all vital organs, estimate $\dot{q}_{vit\ BS}$ of vital organs.

$$\begin{aligned}\dot{q}_{vit\ BS} &= \eta_{eff,Kid,\ BS}\ \dot{q}_{Kid,m,RS-1}\ m_{Kids,BS} + \eta_{eff,H,\ BS}\ \dot{q}_{H,m,RS-1}\, m_{H,BS} + \\ &\eta_{eff,H,\ BS}\, \dot{q}_{Br,m,,RS-1} m_{Br,BS} + \eta_{eff,L,\ BS} \dot{q}_{L,m,,RS-1}\ m_{L,BS},\end{aligned} \tag{31}$$

For BS = dog, $\dot{q}_{vit\ dog}$ = 12.54 W,

Step 6 : Estimate $SOrMR_R$ or $\{\dot{q}_{R,m,\ BS}\}$ for the rest of the organs *R*, which represents the sum of all "minor" organs (e.g., SM, AT, lungs, etc.). Adipose tissue is metabolically inert compared to vital organs [24], 100 times less than the kidney and ten times less than the liver. The $f_{RM,6}$ = -.17 for RM

 doi:10.20944/preprints202503.0386.v1

suggests that decreasing SOrMR$_{RM}$ of RM with increasing body size indicates OD occurs in a few organs within RM.

Using EAR for $\dot{q}_{RM,m,dog}$ = 0.99 W/kg, mRM= 9.35 Kg , $\dot{q}_{RM,dog}$ = 9.24 W

The current work uses both EAR for *R* and Elia's constant values for $\dot{q}_{R,m}$ as 0. 581 W/kg was used to study the extent of the effects of change in $\{\dot{q}_{R,m,\,BS}\}$ on Kleiber's law.

Step 7: Compute the whole-body MR ($\dot{q}_B$):

$$\dot{q}_B = \dot{q}_{vit,BS} + \dot{q}_{R,BS}, \quad \dot{q}_{R,BS} = \dot{q}_{R,m,BS}\, m_R \tag{32}$$

$$\dot{q}_B = 12.54 + 9.24 = 22.6 \text{ W}$$

Step 8: Plot ln vs. ln(M$_B$) for 116 species, with mass ranging from 0.0076 kg to 6,650 kg (order of variation, 10^7). Use: a) EAR for all organs $\dot{q}_{RM,m}$ yielding b = 0.76 and b) EAR for vital organs and Elia's constant for $\dot{q}_{RM,m}$ yielding b = 0.758 (Figure 4).

Step 9: Using ODM for all vital organs, generate SOrMR$_k$ for vital organs, assuming a) EAR for RM $\dot{q}_{RM,m}$, compute and plot ln ($\dot{q}_B$) vs. ln(M$_B$), yielding b = 0.75 and compare with EAR correlations for all organs (Figure 5) b) EAR for vital organs and Elia's constant for $\dot{q}_{RM,m}$ yielding b = 0.77 (Figure 6).

Step 10: Obtain $\dot{q}_{vit}$ using ODM, plot vs. ln(M$_{vit}$) and compare them with literature data (Figure 7); compute as $\frac{\dot{q}_{vit}}{\dot{q}_B} * 100$ and compare with literature data {Figure 8}.

Step 11: For UMR, Set $\eta_{eff,k}$ = 1 for all vital organs and get upper metabolic rate for organs $\dot{q}_{k,m,UMR}$ and $\dot{q}_{B,UMR}$ if $\dot{q}_{RM,m}$ follows a) organ allometric laws, b) isolated rates. Plot $\dot{q}_{B,UMR}$ vs. ln(M$_B$) for 116 species and show that b$_{UMR}$ = 0.86 if $\dot{q}_{RM,m}$ follows organ allometric laws and b$_{UMR}$ = 0.92 if $\dot{q}_{RM,m} = \dot{q}_{RM,m,iso}$ ().

Step 12: For, MMR , use measured perfusion ratio for Kid, H, Br, L, SM and RM-ex to estimate i) lower bound on MMR with increased organ metabolic rates but still with OD gradients, and ii) upper bound on MMR with $\eta_{eff,k}$=1 for Kid, H, Br, Land SM (zero OD gradient). For dog of 10 kg, lower blund MMR= 26.92 W, upper bound on MMR= 94.5 W Plot ln $\dot{q}_{B,MMR}$ v n (M$_B$), show that b$_{MMR}$ =0.798 (lower bound MMR) , 0.94 (upper bound MMR)

References

1. Popovic, M. , " Thermodynamic properties of microorganisms: determination and analysis of enthalpy, entropy, and Gibbs free energy of biomass, cells and colonies of 32 microorganism species,," *Heliyon* , vol. 5, no. e0195, 2019.
2. Popovic M, "Beyond COVID-19: Do biothermodynamic properties allow predicting the future evolution of SARS-CoV-2 variants?,," *Microbial Risk Analysis,*, vol. 22, no. 100232, https://doi.org/10.1016/j.mran.2022.100232., 2022.
3. Annamalai K., "Oxygen Deficient (OD) Combustion and Metabolism: Allometric Laws of Organs and Kleiber's Law from OD Metabolism?,," *Journal: Systems* , vol. 9, no. 54, 34 pages https://doi.org/10.3390/systems9030054, 2021.
4. Kleiber M., "Body size and metabolism.," *Hilgardia. 1932;6:315–353. [Google Scholar]*, vol. 6, no. Hilgardia. 1932;6:315–353. [Google Scholar], pp. 316-353, 1932.

 doi:10.20944/preprints202503.0386.v1

5. Kleiber, M. , The fire of life: An introduction to animal energetics, NY: Krieger, 1961.
6. White C R and Seymour R S ,, "Revew-Allometric scaling of mammalian metabolism," *The Journal of Experimental Biology,* vol. 208, no. The Company of Biologists 2005 doi:10.1242/jeb.01501, pp. 1611-1619 ,, 2005.
7. West GB, Brown JH, Enquist BJ. , "A general model for the origin of allometric scaling laws in biology.," *Science,* vol. 276, no. 5309, doi: 10.1126/science.276.5309.122. PMID: 9082983., pp. 122-126, 1997.
8. Hoppeler H. and Weibel, E R,, "On Scaling functions to body size: theories and facts-Editorial,," *Special Issue is dedicated toThe Journal of Experimental Biology,* vol. 208, no. Special Issue is dedicated to Knut Schmidt-Nielsen,The Company of Biologists,doi:10.1242/jeb.01630, pp. 1573-74, 2005.
9. Banavar, J. R., Maritan, A. & Rinaldo A, "Size and form in efficient transportation networks," *Nature,* vol. 399, pp. 130-132, 1999.
10. Bejan A, In Shape and Structure, from Engineering to Nature, p 260-266, Cambridge: Cambridge: Cambridge University Press., 2000.
11. Bejan A, "The constructal law of organization in nature: tree-shaped flows and body size.," *J Exp Biol . ,* vol. 208, no. 9, doi: https://doi.org/10.1242/jeb.01487, p. 1677–1686, 2005.
12. Singer D., "Size relationship of metabolic rate: oxygen availability as the “missing link” between structure and function?”, Review," *Thermochimica Acta,* vol. 446, no. doi:10.1016/j.tca.2006.05.006, p. 20–28, 2006.
13. Trayhun P. , "Oxygen—A Critical, but Overlooked, Nutrient," *Front. Nutr.,HYPOTHESIS AND THEORY ARTICLE, ,* vol. 6, no. Article 10, https://doi.org/10.3389/fnut.2019.00010, 2019.
14. West, G. B., Brown, J. H. and Enquist, B. J., "The fourth dimension of life: fractal geometry and allometric scaling of organisms.," *Science,* vol. 284, no. Science, pp. 1677-1679., 1999.
15. Painter PR, ".Allometric scaling of the maximum metabolic rate of mammals: oxygen transport from the lungs to the heart is a limiting step.," *Theor Biol Med Model. 11;2:31. doi: 10.1186/1742-4682-2-31. PMID: 16095539; PMCID: PMC1236962.,* vol. 11, no. doi: 10.1186/1742-4682-2-31. PMID: 16095539; PMCID: PMC1236962., 2005.
16. Weibel ER, Hoppeler H, " Exercise-induced maximal metabolic rate scales with muscle aerobic capacity.," *J Exp Biol,* vol. 208, no. 9, . doi: https://doi.org/10.1242/jeb.01548, p. 1635–1644, 2005 .
17. Silva J K L , Garcia G J M , Barbosa L A, , "Allometric scaling laws of metabolism," *Physics of Life Reviews, 3 , 2006, 229–261,* vol. 3, no. , p. 229–261, 2006.
18. Painter, P. , "Rivers, blood and transportation networks.," *Nature* , vol. 408, no. https://doi.org/10.1038/35041631, p. 159, 2000.
19. Demetrius, L., "Demetrius, L.Directionality theory and the evolution of body size.," *Proc. R. Soc. Lond. ,* vol. B 267, pp. 2385-2391., 2000.
20. Wang Z , Zhang J, Ying Z, Heymsfield S. B., "Organ-Tissue Level Model of Resting Energy Expenditure Across Mammals: New Insights into Kleiber’s Law," *International Scholarly Research Network ISRN Zoology.,* no. Article ID 673050, doi:10.5402/2, p. 9 pages , 2012.
21. Wang Z, O'Connor TP, Heshka S, Heymsfield SB., "The reconstruction of Kleiber's law at the organ-tissue level," *J.Nutr.,* vol. 131, pp. 2967-70, 2001.
22. Wang Z, Ying Z, Bosy-Westphal A, Zhang J, Schautz B, Later W., "Specific metabolic rates of major organs and tissues across adulthood: evaluation by mechanistic model of resting energy expenditure," *The American Journal of Clinical Nutrition,* vol. 92(6), 2010,.
23. Gallagher, D.; Belmonte, D.; Deurenberg, P.; Wang, Z.M.; Krasnow, N.; Pisunyer, F.X.; Heymsfield, S.B., "Organ-tissue mass measurement allows modeling of REE and metabolically active tissue mass,," *American Journal of Physiology. Endocrinology and Metabolism,* vol. 38, no. ISSN 0193-1849, Doi: https://doi.org/10.1152/ajpendo.1998.275.2.e249, pp. E249 - E258, 1998.
24. Antoł A, Kozłowski J, , "Scaling of organ masses in mammals and birds: phylogenetic signal and implications for metabolic rate scaling,," *ZooKeys* , vol. 9821, no. doi: 10.3897/zookeys.982.55639, p. 149–159 , 2020.
25. Annamalai K, Ryan W., "Interactive processes in gasification and combustion- I: Cloud of droplets," *Progress in Energy and Combustion Science,* vol. 19, no. 5, pp. 383-446, 1993.

 doi:10.20944/preprints202503.0386.v1

26. Annamalai K, Ryan W.,, "Interactive processes in gasification and combustion- II: Isolated carbon/coal and porous char particles," *Progress in Energy and Combustion Science, vol. 19, no. 5, pp. 383-446, 1993,* vol. 19, no. 5, pp. 383-446, 1993.
27. Annamalai,K., Ryan,W. and Dhanapalan,S., "Interactive processes in gasification and combustion-III: Coal particle arrays, streams and clouds," *Journal of the Progress in Energy and Combustion Science,* vol. 20, no. 6, pp. 487-618, 1994.
28. Kapteijn F, Marin G B, Moulijn J.A., "Catalytic reaction engineering, in Catalysis: an integrated approach," NY, Elsevier, Hardcover ISBN: 9780444829634, 1999.
29. Annamalai K. and Nanda, A., "Biological aging and life span based on entropy stress via organ and mitochondrial metabolic loading," *Entropy,* vol. 19, no. doi:10.3390/e19100566, p. 566, 2017.
30. Elia M., "Organ and tissue contribution to metabolic rate," in *Energy metabolism: tissue determinants and cellular corollaries*, New York, Raven Press, Ltd, 1992, pp. 61-79.
31. Groebe K, " An Easy-to-Use Model for 02 Supply to Red Muscle, Validity of Assumptions, Sensitivity to Errors in Data,," *Biophysical Journal,* vol. 68, no. Biophysical Journal, V 68 , 1995, 1246—1269, p. 1246—1269, 1995.
32. Pias S C, "How does oxygen diffuse from capillaries to tissue, Symposium Review," *J Physiol* , no. 599.6 , pp. 1769-1782, 2021.
33. Singer D, Schunck O, Bach F, Kuhn HJ., "Size effects on metabolic rate in cell, tissue, and body calorimetry.," *Thermochimica Acta,* vol. 251, pp. 227-240, 1995.
34. Place TL, Domann FE, Case AJ., " Limitations of oxygen delivery to cells in culture: An underappreciated problem in basic and translational research.," *Free Radic Biol Med,* vol. 113, no. :doi: 10.1016/j.freeradbiomed.2017.10.003. Epub 2017 Oct 13. Errat, pp. 311-322, 2017.
35. Schumacker PT, Samsel RW, "Analysis of oxygen delivery and uptake relationships in the Krogh tissue model. J Appl Physiol (1985). 1989 Sep;67(3):1234-44. doi: 10.1152/jappl.1989.67.3.1234. PMID: 2793716.," *J Appl Physiol (1985). 1989 Sep;67(3):1234-44. doi: 10.1152/jappl.1989.67.3.1234. PMID: 2793716.*, vol. 67, no. doi: 10.1152/jappl.1989.67.3.1234. PMID: 2793716., pp. 1234-44, 1989.
36. Wheaton WW, Chandel NS., " Hypoxia. 2. Hypoxia regulates cellular metabolism.," *Am J Physiol Cell Physiol.,* vol. 300 , no. 3, doi: 10.1152/ajpcell.00485.2010. Epub 2010 Dec 1. PMID: 21123733; PMCID: PMC3063979, pp. C385-93. , 2011.
37. WANG, R., HUSSAIN, A., GUO, Q., JIN, X., WANG, M.., "Oxygen and Iron Availability Shapes Metabolic Adaptations of Cancer Cells.," *World Journal of Oncology, North America,* , no. Available at: <https://www.wjon.org/index.php/wjon/article/view/1739/149, 2024.
38. Melkonian EA, Schury MP., " Biochemistry, Anaerobic Glycolysis. [Updated 2023 Jul 31].," Treasure Island (FL), In: StatPearls [Internet]. StatPearls Publishing;; Available from: https://www.ncbi.nlm.nih.gov/books/NBK546695/, 2024.
39. Zheng J. , "Energy metabolism of cancer: Glycolysis versus oxidative phosphorylation (Review).," *Oncol Lett. 2012 Dec;4(6):1151-1157. doi: 10.3892/ol.2012.928. Epub 2012 Sep 20. PMID: 23226794; PMCID: PMC3506713.*, vol. 4 , no. doi: 10.3892/ol.2012.928. Epub, pp. 1151-1157., 2012.
40. Avaiabke online https://www.webmd.com/cancer/cancer-incidence-age (accessed on 11/19/2024.
41. Accesed on 09/10/2024, Ratcliffe group | Hypoxia biology in cance; Accessed 06/17/2024 https://www.ck12.org/book/human-biology-circulation/section/5.1/].
42. Grant H et.al. and 18 other authors, "Larger organ size caused by obesity is a mechanism for higher cancer risk," *bioRxiv,* no. 2020.07.27.223529; doi: https://doi.org/10.1101/2020.07.27.223529, 2020.
43. Piiper P, Scheid J., "Cross-sectional PO2 distributions in Krogh cylinder and solid cylinder models," *Respir Physiol,* vol. 64, pp. 241-251, 1986.
44. Smil V, "Laying down the law, Millennium Essay," *Nature,* vol. 403, no. www.nature.com, p. 597, 2000.
45. Morisaki H , Sibbald W J , "Tissue oxygen delivery and the microcirculation,,,," *Critical Care Clinics,* vol. 20, no. 2, https://doi.org/10.1016/j.ccc.2003.12.003., pp. 213-223, 2004.
46. Ostergaard L, , " Blood flow, capillary transit times, and tissue oxygenation: the centennial of capillary recruitment,," *Journal of Applied Physiology 129:6, 1413-1421,* vol. 129, no. 6, pp. 1413-1421, 2020.

 doi:10.20944/preprints202503.0386.v1

47. A.M. Makarieva, V.G. Gorshkov, B. Li, S.L. Chown, P.B. Reich, V.M. Gavrilov, , "Mean mass-specific metabolic rates are strikingly similar across life's major domains: Evidence for life's metabolic optimum," *Proc. Natl. Acad. Sci. U.S.A.,* vol. 105 (44), no. 44, , pp. 16994-16999, .
48. A.M. Makarieva, V.G. Gorshkov, B. Li, S.L. Chown, P.B. Reich, V.M. Gavrilov,, "Mean mass-specific metabolic rates are strikingly similar across life's major domains: Evidence for life's metabolic optimum,," *Proc. Natl. Acad. Sci. U.S.A.,* vol. 105, no. 44, 16994-16999, https://doi.org/10.1073/pnas.0802148105 (2008), 2008.
49. Lindstedt SL, Schaeffer PJ., " Use of allometry in predicting anatomical and physiological parameters of mammals.," *Lab Anim.* , vol. 36, no. 1; . doi: 10.1258/0023677021911731. PMID: 11833526., pp. 1-19, 2002.
50. Holliday M A , Potter, D, Arrah A and Beard S,, " The Relation of Metabolic Rate to Body Weight and Organ Size, A Review ,," *Pediat. Res.,* vol. 1, pp. 185-195, 1967 Pediat. Res. 1: 185-195 (1967).
51. shcroft S P, Stocks B, Egan B , Zierath J R , " Exercise induces tissue-specific adaptations to enhance cardiometabolic health,," *Cell Metabolism,,* vol. 36, no. 2, https://doi.org/10.1016/j.cmet.2023.12.008, , pp. 278-300, 2024.
52. Wendt, D., van Loon, L.J. & Marken Lichtenbelt, W.D., " Thermoregulation during Exercise in the Heat.," *Sports Med* , vol. 37, no. https://doi.org/10.2165/00007256-200737080-00002, pp. 669–682 https://doi.org/10.2165/00007256-200737080-00002, 2007.
53. DELMAR R. FINCO, , " Chapter 9 Kidney Function, KANEKO,J R , editor,," in *Clinical Biochemistry of Domestic Animals (Third Edition),*, Academic Press,,ISBN 9780123963505,, https://doi.org/10.1016/B978-0-12-396350-5.50014-0., 1980, pp. 337-400,.
54. Joyner M J and Casey D P, "Regulation of Increased Blood Flow (Hyperemia) to Muscles During Exercise: A Hierarchy of Competing Physiological Needs,," *Physiological Reviews,* vol. 95, no. 2, pp. 549-601, 2015.
55. Angleys, H , Østergaard, L, "Krogh's capillary recruitment hypothesis, 100 years on: Is the opening of previously closed capillaries necessary to ensure muscle oxygenation during exercise?," *American Journal of Physiology-Heart and Circulatory Physiology,* no. doi: 10.1152/ajpheart.00384.2019, pp. 318, H425-H447, 2019.
56. Heinonen, I, Kalliokoski K, K Hannukainen,J C , Duncker D J , Nuutila,P and Knuuti J ,, "Organ-Specific Physiological Responses toAcuteP hysical Exercise and Long-Term Trainingi n Humans,," *Int.Union Physiol.Sci., Am.Physiol.Soc. Physiology 29:421–436,2014;doi:10.1152/physiol.00067.2013,* vol. 20, no. ;doi:10.1152/physiol.00067.2013, pp. 421-436, 2014.
57. Wasserman DH, Cherrington AD., " Hepatic fuel metabolism during muscular work: role and regulation.," *Am J Physiol.: doi: 10.1152/ajpendo.1991.260.6.E811. PMID: 2058658.,* vol. 260(6 Pt 1), no. doi: 10.1152/ajpendo.1991.260.6.E811. PMID: 2058658.; https://pubmed.ncbi.nlm.nih.gov/2058658/, pp. E811-24., 1991.
58. Barbosa L A ,Garcia G J M , da Silva J K L,, "The scaling of maximum and basal metabolic rates of mammals and birds, Physica A: Statistical Mechanics and its Applications,," vol. 359, no. https://doi.org/10.1016/j.physa.2005.06.050., pp. 547-554, 2006.
59. Accessed on 12/21/2024 https://health.howstuffworks.com/wellness/diet-fitness/exercise/sports-physiology8.htm, posted by By: Craig Freudenrich, Ph.D..
60. Smith K J and Ainslie P N,, " Regulation of cerebral blood flow and metabolism during exercise," *Exp Physiol* , vol. 102, no. 11 , p. 1356–1371, 2017.
61. Ahulwalia A., "Allometric scaling in-vitro, Scientific Reports, 7:42113 | DOI: 10.1038/srep42113," www.nature.com/scientificreports, 2017.
62. Prange H D , Anderson J F and Rahn H, "Scaling of Skeletal Mass to Body Mass in Birds and Mammals, T," *he American Naturalist,* vol. 113, no. 1, pp. 103-12, 1979.
63. Kayser, C., and A. Heusner. 1964., "Etude comparative du metabolism &Energetique dans la s&rie animale.," *J. Physiol. (Paris),* vol. 56, pp. 489-524, 1964.
64. White, "Metabolic Scaling in Animals: Methods, Empirical," no. DOI: 10.1002/cphy.c110049, 2014.
65. Midorikawa T, Tanaka S, Ando T, Tanaka C, Masayuki K, Ohta M, Torii S, Sakamoto S, "Is There a Chronic Elevation in Organ-Tissue Sleeping Metabolic Rate in Very Fit Runners?," *Nutrients,* vol. 8, no. 4, doi: 10.3390/nu8040196. PMCID: PMC4848665., p. 196. , 2016.

 doi:10.20944/preprints202503.0386.v1

66. Korthuis RJ., "Skeletal Muscle Circulation. Ed. San Rafael (CA)," in *Chapter 4, Exercise Hyperemia and Regulation of Tissue Oxygenation During Muscular Activity.*, Morgan & Claypool Life Sciences;, Available from: https://www.ncbi.nlm.nih.gov/books/NBK57139/, 2011.
67. Tayor et al , "Resp Physio," vol. 44, pp. 25-37, 1981.
68. Weibel ER, Bacigalupe LD, Schmitt B, Hoppeler H. , "Allometric scaling of maximal metabolic rate in mammals: muscle aerobic capacity as determinant factor.," *Resp Physiol Neurobiol,* vol. 140, p. 115–32., 2004.
69. De Moraes R, Gioseffi G, Nóbrega AC, Tibiriçá E., "Effects of exercise training on the vascular reactivity of the whole kidney circulation in rabbits.," *J Appl Physiol,* vol. 97, no. doi: 10.1152/japplphysiol.00923.2003, pp. 683-8, 1985.
70. Poortmans JR., " Exercise and renal function.1," *Sports Med.1,* vol. 1, no. 2 doi: 10.2165/00007256-198401020-00003. PMID: 6567229., pp. 125-53, 1984.
71. Lindstedt SL, Hoppeler H. , "Allometry: revealing evolution's engineering principles.," *J Exp Biol. ,* vol. 226, no. 24; jeb245766. doi: 10.1242/jeb.245766. Epub 2023 Dec 11. PMID: 38078372., 2023.
72. Agutter PS, Wheatley DN. , "Metabolic scaling: consensus or controversy?. ;1:13. Published 2004 Nov 16. doi:10.1186/1742-4682-1-13," *Theor Biol Med Model. ,* no. 13, doi:10.1186/1742-4682-1-13, 2004.
73. Pryce, and 11 additional authors, "Reference ranges for organ weights of infants at autopsy: Results of >1,000 consecutive cases from a single centre.," *BMC clinical pathology,* vol. 14, no. DOI: 10.1186/1472-6890-14-18, p. 18, 2014.
74. Packard, G.C. , "Rethinking the metabolic allometry of ants. Evol Ecol 34, 149–161 (2020). https://doi.org/10.1007/s10682-020-10033-5," *Evol Ecol,* vol. 34, no. https://doi.org/10.1007/s10682-020-10033-5, p. 149–161 , 2020.
75. Dawson TH., "Scaling laws for capillary vessels of mammals at rest and in exercise," *Proc. R. Soc. Lond. B,* vol. 270, no. DOI 10.1098/rspb.2002.2304, p. 755–763, 2003.
76. Hulbert A J, "A Sceptics View: “Kleiber’s Law” or the “3/4 Rule” is neither a Law nor a Rule but Rather an Empirical Approximation," *Systems,* vol. 2, no. doi:10.3390/systems2020186 OPEN ACCESS , systems , ISSN 2079-8954, pp. 186-202, 2014.
77. Krebs AH., "Body size and tissue respiration," *Biochem. et Biophys. Acta,* vol. 4, pp. 249-269, 1950.
78. Porter RK., "Allometry of mammalian cellular oxygen consumption," *Cell. Mol. Life Sci.,* vol. 58, p. 815–822., 2001.
79. Gutierrez WR., "xSite model of allometric scaling and fractal distribution networks of organs," [https://arxiv.org/pdf/q-bio/0404039], accceesed Feb 26 2019.
80. Later W, Bosy-Westphal A, Hitze B, Kossel E, Glüer CC, Heller M, Müller MJ. , "No evidence of mass dependency of specific organ metabolic rate in healthy humans.," *Am J Clin Nutr.,* vol. 4, no. doi: 10.1093/ajcn/88.4.1004. PMID: 18842787., pp. 1004-9, 2008.
81. Glazier D S , "Beyond the ’3/4-power law’: variation in the intra- and interspecific scaling of metabolic rate in animals," . *Biological Reviews,* vol. 80, no. DOI: https://doi.org/10.1017/S1464793105006834, PMID: 16221332, pp. 611-662, 2005.
82. Glazier, D.S. , "Body-Mass Scaling of Metabolic Rate: What are the Relative Roles of Cellular versus Systemic Effects?," *Biology,* vol. 4, no. https://doi.org/10.3390/biology4010187, pp. 187-199., 2015.
83. Carreau A, El Hafny-Rahbi B, Matejuk A, Grillon C, Kieda C., " Why is the partial oxygen pressure of human tissues a crucial parameter? Small molecules and hypoxia.," *J Cell Mol Med. ,* vol. 15, no. 6, doi: 10.1111/j.1582-4934.2011.01258.x. PMID: 21251211, pp. 1239-53, 2011.
84. Wagner BA, Venkataraman S, Buettner GR., " The rate of oxygen utilization by cells.," *Free Radic Biol Med. ,* vol. 51, no. 3, doi:10.1016/j.freeradbiomed.2011.05.024, pp. 700-712., 2011.
85. Savage VM, Allen AP, Brown JH, Gillooly JF, Herman AB, Woodruff WH, West GB. , "Scaling of number, size, and metabolic rate of cells with body size in mammals.," *Proc Natl Acad Sci U S A.,* vol. 104, no. doi: 10.1073/pnas.0611235104. Epub 2007 Mar, pp. 4718-23, 2007.
86. W. Ryan, K. Annamalai and J. Caton,, "Relation between Group Combustion and Drop Array Studies,," *Combustion and Flame,* vol. 80, pp. 313-321, 1990.
87. Hess; J R, " Diffusion-limited oxygen delivery.," *Blood,* vol. 143, no. 8, doi: https://doi.org/10.1182/blood.2023023201, p. 659–660, 2024.

 doi:10.20944/preprints202503.0386.v1

88. White C R , Seymour R S, "Mammalian basal metabolic rate is propor- tional to body mass 2/3,," *Proc. Natl. Acad. Sci.,* vol. 100, no. Proc. Natl. Acad. Sci. 100 (2003) 4046–4049, pp. 4046-49, 2003.
89. Dodds, P S, Rothman D.H., Weitz J S, "Re-examination of the "3/4-law" of metabolism,," *J. Theor. Biol.,* vol. 209, pp. 9-27, 2001.
90. White C R and Seymour R S , "Revew-Allometric scaling of mammalian metabolism, T," *he Journal of Experimental Biology,* vol. 208, no. The Company of Biologists, doi:10.1242/jeb.01501, pp. 1611-1619 , 2005.
91. Lee SY, Gallagher D., "Assessment methods in human body composition.," *Curr Opin Clin Nutr Metab Care.,* vol. 5, no. doi: 10.1097/MCO.0b013e32830b5f23. PMID: 18685451; PMCID: PMC2741386., pp. 566-72, 2008.
92. "Scaling of Skeletal Mass to Body Mass in Birds and Mammals".
93. Heymsfield S B , Gallagher D, Kotler D P, Wang Z , Allison D B , Heshka S, ",ody-size dependence of resting energy expenditure can".
94. Heymsfield S B , Gallagher D, Kotler D P, Wang Z , Allison D B , Heshka S, "Body-size dependence of resting energy expenditure can be attributed to nonenergetic homogeneity of fat-free mass,," *Am J Physiol Endocrinol Metab , 282: E132±E138, 2002.,* vol. 282, p. E132: E138, 2002.
95. Available online: https://www.cancer.gov/about-cancer/causes-prevention/risk/age#:~:text=Age%20and%20Cancer%20Risk,-Advancing%20age%20is&text=The%20incidence%20rates%20for%20cancer,groups%2060%20years%20and%20older.(accessed on 17th Nov 2024).
96. Sarelius I and U. Pohl, "Control of muscle blood flow during exercise: Local factors and integrative mechanisms,," *Acta Physiologica ,* vol. 199, no. 4, DOI: 10.1111/j.1748-1716.2010.02129.x, pp. 349-65, 2010.
97. Groebe, K, "An Easy-to-Use Model for 02 Supply to Red Muscle, Validity of Assumptions, Sensitivity to Errors in Data,," *Biophysical Journal,,* vol. 68, p. 1246—1269, 1995.
98. Accessed 12/25/2024 https://www.physio-pedia.com/VO2_Max#:~:text=The%20simplest%20formula%20to%20calculate,mL/kg/min)
99. Javed F, He Q, Davidson LE, Thornton JC, Albu J, Boxt L, Krasnow N, Elia M, Kang P, Heshka S, Gallagher D., "Brain and high metabolic rate organ mass: contributions to resting energy expenditure beyond fat-free mass.," *Am J Clin Nutr.,* vol. 4, no. doi: 10.3945/ajcn.2009.28512. Epub 2010 Feb 17. PMID: 20164308; PMCID: PMC2844678., pp. 907-912, 2010.
100. Melzer, "Carbohydrate and fat utilization during rest and physical activity," *The European e-Journal of Clinical Nutrition and Metabolism,* vol. 6, 2011.
101. Hryvniak D, Wilder R P, Jenkins J , Statuta S , ", Chapter 15 - Therapeutic Exercise, Editor(s): David X. Cifu,," in *Braddom's Physical Medicine and Rehabilitation (Sixth Edition),* NY, Elsevier , https://doi.org/10.1016/B978-0-323-62539-5.00015-1., 2011, pp. 291-315,.